DEVELOPMENT OF MODELS FOR RATING SEISMIC ACTIVITIES USING RADIATED ENERGY OF EARTHQUAKES

BY

OLUMIDE AKINWALE ADEDEJI

B.Sc. (Hons), M.Sc. Physics (Ibadan)

Matric. N0. 63688

A Thesis in the Department of Physics,

Submitted to the Faculty of Science

in partial fulfillment of the requirements for the Degree of

DOCTOR OF PHILOSOPHY

of the

UNIVERSITY OF IBADAN

July 2012

CERTIFICATION

I certify that this work was carried out under my supervision by **Mr. Olumide Akinwale ADEDEJI** in the Department of Physics, University of Ibadan, Ibadan, Nigeria.

____

SUPERVISOR

Dr. O. I. Popoola
B.Sc., M.Sc., Ph.D (Ibadan)
Senior Lecturer
Department of Physics
University of Ibadan

DEDICATION

THE LORD, MY SHEPHERD.

ACKNOWLEDGEMENT

"The desire accomplished is sweet . . ." Solomon David-Jesse.

On this note, I sincerely appreciate the great efforts of my Supervisor, Dr. Olatunde Isaiah Popoola at every stage of this research work. His keenness, regular and systematic logic coupled with high-level of technical, scientific and academic rigour have provided adequate and sufficient exposure needed for this work. It's always a great priviledge to learn from you.

This work has benefited from the wealth of academics experience of the leadership of the department as well as all the participants of the weekly Physics Department Academic Seminars for their valuable comments and constructive criticisms during my previous presentations. Special thanks to Professor I.P. Farai, Professor E.O. Oladiran, Dr. F.O. Ogundare, Dr. O.E. Awe, Dr. Adetoyinbo and Dr. Adegoke for providing continuous feedback and valuable advice throughout the period of this work.

I will always appreciate my dearest friend, Dr. Omololu AkinOjo for his great assistance and moral support.

My dearest wife, Foluso and my lovely children, Andersen and Kelvin made sacrifices during my long hours of research and working. My lovely parent, Pa Emmanuel Olasupo Adedeji and Mrs. Olanike Oluwayemisi Adedeji, laid the solid foundation, through God's Grace, for me to be here today. I'll always love you. My siblings (Kemi, Folake and Lekan) have always been wonderful, making us a four-strong-fold.

I am very grateful to the Northern California Earthquake Data Centre for granting access to their website to download data for this work.

Various authors and institutions have assisted in great measure to the completion of this work. They are listed in the references. I appreciate your sharing of scientific knowledge toward the growth of mankind.

Finally, I submit to the Lord, my Shepherd for His Love, Goodness, Mercy, Grace and Provisions all through and through.

Olumide Akinwale Adedeji

July 2012

ABSTRACT

Seismic activity evaluation is usually carried out using the Gutenberg-Richter's (G-R) relation. This relation is defective because it does not include area of the region involved, thereby making a small but active region to be underrated. Secondly it gives the rate of seismicity of a region in terms of the total number, N, of earthquakes irrespective of magnitudes. This makes regions with few but great earthquakes to be underestimated since energy due to magnitude m is proportional to 10^m. Therefore the method does not justifiably compare seismic activities of two or more regions. Assessment of seismic activities of regions in terms of radiated energy of earthquakes will make comparison reliable because each earthquake magnitude will be converted to its equivalent energy. The aim of this work was to develop models for rating seismic activities in terms of radiated energy of earthquakes.

Considering an arbitrary region of area A where N earthquakes have occurred over a period T, total radiated energy per unit area per unit time was defined as $\Im = \sum_{i}^{N} E_i / TA$; where E_i is the energy radiated by the ith earthquake. The E_i was expressed in terms of earthquake moment magnitude, m_i, as $E_i = 10^{(1.5m_i + 11.8)}$ using Bath equation to yield the first model $\Im_1$. A second model, $\Im_2$, was developed by dividing T into equal sub-periods, and substituting for m in the G-R relation. Fifty-year (1956 - 2005) earthquake data for 10 regions in the world seismic zones were obtained from the Catalogue of Advanced National Seismic System (ANSS), U.S.A. The regions were Mediterranean (Rg1), Southern Africa (Rg2), West Europe (Rg3), West Pacific (Rg4), South Australia (Rg5), Southwest Pacific (Rg6), West of South America (Rg7), West of North America (Rg8), Arctic (Rg9) and Japan (Rg10). Different magnitude types of the data were converted to moment magnitudes using empirical relations of Geller and Kanamori. The G-R relation and the developed models were applied to each region.

The developed models were $\Im_1 = \frac{1}{50}\sum_{i=1}^{k} \frac{10^{(1.5m_i + 11.8)}}{A}$ and $\Im_2 = \frac{1}{50A}\sum_{j=1}^{5} \frac{10^{1.5a_j/b_j}}{N_j^{1/b_j}} \times 10^{11.8}$ where k is the total number of earthquakes in a region; a_j and b_j are G-R constants for the jth sub-period. The average values of G-R constant, a, obtained for regions 1 to 10 were 6.20, 5.06, 3.37, 4.44, 4.56, 5.19, 3.52, 3.95, 6.20, and 3.72. Thus, the G-R rated the regions as Rg3 < Rg7 < Rg10 < Rg8 < Rg4 < Rg6 < Rg5< Rg2 < Rg9< Rg1.

The respective values of $\Im_1$ and $\Im_2$ for regions 1 to 10 in 10^{11} J $km^{-2}yr^{-1}$ were 1.37 and 6.29; 0.08 and 2.07; 0.40 and 3.15; 0.81 and 6.21; 0.65 and 5.16; 0.72 and 5.39; 0.53 and 4.15; 0.22 and 3.04; 0.22 and 3.05; 3.76 and 8.36. Both models rated the regions as Rg2<Rg8<Rg9<Rg3<Rg7<Rg5<Rg6<Rg4<Rg1<Rg10.

The two models gave a more reliable seismic activity rating than Gutenberg-Richter's relation. The first Model is suitable for all categories of magnitude spread including those for which Gutenberg-Richter's constants are indeterminate while the second model will not be applicable when Gutenberg-Richter's constants are indeterminate.

Keywords: Seismic activities, Gutenberg-Richter's relation, Earthquakes, Radiated energy.

Word Count: 487.

TABLE OF CONTENTS

LIST OF TABLES

LIST OF FIGURES

Definition of Terms

Aftershock:

An earthquake that follows a larger earthquake or main shock and originates at or near the focus of the larger earthquake. Generally, major earthquakes are followed by a larger number of aftershocks, decreasing in frequency with time.

Amplitude:

The maximum height of a wave crest or depth of a trough.

Array:

An ordered arrangement of seismometers or geophones, the data from which feeds into a central receiver.

Arrival:

The appearance of seismic energy on a seismic record.

Arrival time:

The time at which a particular wave phase arrives at a detector.

Aseismic:

Unassociated with an earthquake.

Asthenosphere:

The layer of mantle underlying the lithosphere which is close to its melting point and therefore much less rigid than the lithosphere.

Body wave:

A seismic wave that travels through the interior of the earth and is not related to a boundary surface.

Continental Crust:

Outermost solid layer of the earth that forms the continents and is composed of igneous, metamorphic, and sedimentary rocks. Overall, the continental crust is broadly granitic in composition. Contrast with oceanic crust.

Continental Drift:

The theory, first advanced by Alfred Wegener, that the earth's continents were originally one land mass called Pangaea. About 200 million years ago Pangaea split off and the pieces migrated (drifted) to form the present-day continents. The predecessor of plate tectonics.

Crust:

The outer layer of the earth's surface.

Dilatancy:

An increase in the bulk volume of rock during deformation. Possibly related to the migration of water into microfractures or pores.

Divergent Plate Boundary:

The boundary between two crustal plates that are pulling apart (e.g. sea floor spreading).

Earthquake:

Shaking of the earth caused by a sudden movement of rock beneath its surface.

Earthquake swarm:

A series of minor earthquakes, none of which may be identified as the main shock, occurring within a limited area and time.

Elastic wave:

A wave that is propagated by some kind of elastic deformation, that is, a deformation that disappears when the forces are removed. A seismic wave is a type of elastic wave.

Epicenter:

That point on the earth's surface directly above the hypocenter of an earthquake.

Fault:

A weak point in the earth's crust where the rock layers have ruptured and slipped.

First arrival:

The first recorded signal attributed to seismic wave travel from a known source.

Focal zone:

The rupture zone of an earthquake. In the case of a great earthquake, the focal zone may extend several hundred kilometers in length.

Focus:

That point within the earth from which originates the first motion of an earthquake and its elastic waves.

Foreshock:

A small tremor that commonly precedes a larger earthquake or main shock by seconds to weeks and that originates at or near the focus of the larger earthquake.

Harmonic Tremor:

A continuous release of seismic energy typically associated with the underground movement of magma, often preceding volcanic eruptions. It contrasts distinctly with the sudden release and rapid decrease of seismic energy associated with the more common type of earthquake caused by slippage along a fault.

Hypocenter:

The calculated location of the focus of an earthquake.

Igneous:

As in igneous rock. A rock formed when magma, or molten rock, cools and solidifies. If it cools slowly, the rock will have a coarse crystalline texture. If it cools quickly, it will have a fine crystalline texture. If it cools very quickly ("quenched"), it forms a glass, which has no crystalline structure. The three main types of rocks are sedimentary, igneous and metamorphic.

Intensity:

A measure of the effects of an earthquake at a particular place on humans and/or structures. The intensity at a point depends not only upon the strength of the earthquake (magnitude) but also upon the distance from the earthquake to the epicenter and the local geology at that point.

Isoseismal line:

A line connecting points on the earth's surface at which earthquake intensity is the same. It is usually a closed curve around the epicenter.

Leaking mode:

A surface seismic wave which is imperfectly trapped so that its energy leaks or escapes across a layer boundary causing some attenuation.

Lg Wave:

A surface wave that travels through the continental crust.

Liquefaction:

The process in which a solid (such as soil) takes on the characteristics of a liquid as a result of an increase in pore pressure and a reduction in stress. In other words, solid ground turns to jelly.

Lithosphere:

The rigid crust and uppermost mantle of the earth. Thickness is on the order of 62 miles (100 kilometers). It is stronger than the underlying asthenosphere.

Love wave:

A major type of surface wave having a horizontal motion that is shear or transverse to the direction of propagation. It is named after A.E.H. Love, the English mathematician who discovered it.

Low-velocity zone:

Any layer in the earth in which seismic wave velocities are lower than in the layers above and below. More commonly the "slow" layer just beneath the lithosphere.

Magma:

Molten rock beneath the surface of the earth. Molten rock erupted at the surface is termed "lava."

Magnitude:

A quantitative measure of the strength of an earthquake. Magnitude is calculated from ground motion as measured by seismograph and incorporates the distance of the seismograph from the earthquake epicenter so that, theoretically, the magnitude calculated for an earthquake would be the same from any seismograph station recording that earthquake. This is a logarithmic value originally defined by Wadati (1931) and Richter (1935). An increase of one unit of magnitude (for example, from 4.6 to 5.6) represents a 10-fold increase in wave amplitude on a seismogram or approximately a 30-fold increase in the energy released. In other words, a magnitude 6.7 earthquake releases over 900 times (30 times 30) the energy of a 4.7 earthquake - or it takes about 900 magnitude 4.7 earthquakes to equal the energy released in a single 6.7 earthquake! There is no beginning nor end to this scale. However, rock mechanics seem to preclude earthquakes smaller than about -1 or larger than about 9.5. A magnitude -1.0 event releases about 900 times less energy than a magnitude 1.0 quake. Except in special circumstances, earthquakes below magnitude 2.5 are not generally not felt by humans. See also Richter scale.

Major earthquake:

An earthquake having a magnitude of 7 or greater on the Richter scale.

Mantle:

The layer of rock that lies between the outer crust and the core of the earth. It is approximately 1,802 miles (2,900 kilometers) thick and is the largest of the earth's major layers.

Metamorphic:

As in metamorphic rock. A rock formed from any other type of rock by elevated temperatures and pressures, but which has not undergone complete melting. Two common examples of metamorphic rocks are slate (usually formed from shale), and marble (formed from limestone). The three main types of rocks are sedimentary, igneous and metamorphic.

Micro earthquake:

An earthquake having a magnitude of 2 or less on the Richter scale.

Microseism:

A more or less continuous motion in the earth that is unrelated to an earthquake and that has a period of 1.0 to 9.0 seconds. It is caused by a variety of natural and artificial agents.

Modified Mercalli Scale:

Mercalli intensity scale modified for North American conditions. A scale, composed of 12 increasing levels of intensity that range from imperceptible shaking to catastrophic destruction, designated by Roman numerals. It does not have a mathematical basis; instead it is an arbitrary ranking based on observed effects. Contrast with Richter scale, a type of magnitude scale.

Mohorovicic discontinuity:

The boundary surface or sharp seismic-velocity discontinuity that separates the earth's crust from the underlying mantle.

Oceanic crust:

The outermost solid layer of Earth that underlies the oceans. Composed of the igneous rocks basalt and gabbro, and therefore basaltic in composition. Contrast with continental crust.

P (Primary) wave:

Also called compressional or longitudinal waves, P waves are the fastest seismic waves produced by an earthquake. They oscillate the ground back and forth along the direction of wave travel, in much the same way as sound waves (which are also compressional), move the air back and forth as the waves travel from the sound source to a sound receiver.

Pangaea:

The supercontinent composed of all the present-day continents, which existed about 200 million years ago. Continental drift refers to the breakup of Pangaea into the present configuration of continents.

Phase:

The onset of a displacement or oscillation on a seismogram indicating the arrival of a different type of seismic wave.

Plate:

Pieces of crust and brittle uppermost mantle, perhaps 100 kilometers thick and hundreds or thousands of kilometers wide, that cover the earth's surface. The plates move very slowly over, or possibly with, a viscous layer in the mantle at rates of a few centimeters per year.

Plate boundary:

The place where two or more plates in the earth's crust meet.

Plate tectonics:

A widely accepted theory that relates most of the geologic features near the earth's surface to the movement and interaction of relatively thin rock plates. The theory predicts that most earthquakes occur when plates move past each other.

Rayleigh wave:

A type of surface wave having a retrograde, elliptical motion at the earth's surface, similar to the waves caused when a stone is dropped into a pond. These are the slowest, but often the largest and most destructive, of the wave types caused by an earthquake. They are usually felt as a rolling or rocking motion and in the case of major earthquakes, can be seen as they approach. Named after Lord Rayleigh, the English physicist who predicted its existence.

Recurrence interval:

The approximate average length of time between earthquakes in a specific seismically active area.

Richter magnitude scale:

The system used to measure the strength or magnitude of an earthquake. The Richter magnitude scale was developed in 1935 by Charles F. Richter of the California Institute of Technology as a collection of mathematical formulas to compare the size of earthquakes. A similar scale was developed in 1931 by Wadati, so it is more appropriate to call such scales "Wadati-Richter" scales. The magnitude of an earthquake is determined from the logarithm of the amplitude of waves recorded by seismographs. Adjustments are included for the variation in the distance between the various seismographs and the epicenters of the earthquakes. On the Richter Scale, magnitude is expressed in whole numbers and decimal fractions. For example, a magnitude 5.3 might be computed for a moderate earthquake, and a strong earthquake might be rated as magnitude 6.3. Because of the logarithmic basis of the scale, each whole number increase in magnitude represents a tenfold increase in measured amplitude; as an estimate of energy, each whole number step in the magnitude scale corresponds to the release of about 31 times more energy than the amount associated with the preceding whole number value.

Rift system:

The oceanic ridges formed where tectonic plates are separating and new crust is being created; also refers to the on-land counterparts such as the East African Rift.

Ring of Fire:

A 40,000 kilometer (24,855 mile) band of seismicity including mountain-building, earthquakes, and volcanoes, stretching up the west coasts of South and Central America and from the North American continent to the Aleutians, Japan, China, the Philippines, Indonesia, and Australasia.

Rupture zone:

The area of the earth through which faulting occurred during an earthquake. For very small earthquakes, this zone could be the size of a pinhead, but in the case of a great earthquake, the rupture zone may extend several hundred kilometers in length and tens of kilometers in width.

S (secondary or shear) wave:

A seismic body wave that involves particle motion from side to side, perpendicular to the direction of wave propagation. S-waves are slower than P-waves and cannot travel through a liquid such as water or molten rock.

Seafloor Spreading:

The mechanism by which new oceanic crust is created at oceanic ridges and slowly spreads away as the plates separate.

Sedimentary:

As in sedimentary rock. A rock made up of sediments, or rock fragments, laid down in water or deposited by wind or ice. The fragments can be microscopic, like the clays in a shale, or large, like the boulders in a coarse conglomerate. Sandstone, shale, and limestone are common sedimentary rocks. About 70% of the earth's crust is covered with sedimentary rocks (covering igneous or metamorphic rocks). The three main types of rocks are sedimentary, igneous and metamorphic.

Seiche:

A free or standing wave oscillation of the surface of water in an enclosed basin that is initiated by local atmospheric changes, tidal currents, or earthquakes. Similar to water sloshing in a bathtub.

Seismic:

Of or having to do with earthquakes.

Seismic belt:

An elongated earthquake zone, for example, circum-Pacific, Mediterranean, Rocky Mountain. About 75% of the world's earthquakes occur in the circum-Pacific seismic belt.

Seismic constant:

In building codes dealing with earthquake hazards, an arbitrarily-set acceleration value (in units of gravity) that a building must withstand.

Seismicity:

Earthquake activity.

Seismic sea wave:

A tsunami generated by an undersea earthquake.

Seismic zone:

A region in which earthquakes are known to occur.

Seismogram:

A written record of an earthquake, recorded by a seismograph.

Seismograph:

An instrument that records the motions of the earth, especially earthquakes.

Seismograph station:

A site at which one or more seismographs are set up and routinely monitored.

Seismologist:

A scientist who studies earthquakes.

Seismology:

The study of earthquakes and earthquake waves.

Seismometer:

The part of a seismograph which actually senses ground motion, ground velocity or ground acceleration.

Strike-slip fault:

A nearly vertical fault with side-slipping displacement.

Subduction:

The process in which one lithospheric plate collides with and is forced down under another plate and drawn back into the earth's mantle.

Subduction zone:

The zone of convergence of two tectonic plates, one of which is subducted beneath the other. An elongated region along which a plate descends relative to another plate, for example, the descent of the Nazca plate beneath the South American plate along the Peru-Chile Trench.

Surface waves:

Waves that move over the surface of the earth. Rayleigh and Love waves are surface waves.

Tectonic:

Pertaining to the forces involved in the deformation of the earth's crust, or the structures or features produced by such deformation.

Transform Fault:

A plate boundary where one plate slides past another; essentially a large strike-slip fault.

Tremor:

Low amplitude, continuous earthquake activity commonly associated with magma movement.

Tsunami:

One or a series of great sea waves produced by a submarine earthquake, volcanic eruption, or large landslide. (Referred to incorrectly by many as a tidal wave, but these waves have nothing to do with tides). The word tsunami is Japanese for "harbor wave."

CHAPTER ONE

INTRODUCTION

1.1 Earthquakes

An earthquake is the result of a sudden release of energy in the Earth's crust that creates seismic waves. The energy released during an earthquake could be in the form of elastic strain energy, gravitational potential energy or chemical energy. Of all these, the release of elastic strain is the most important cause, because this form of energy is the only kind that can be stored in sufficient quantity in the Earth to produce major disturbances. Earthquakes associated with this type of energy release are called tectonic earthquakes. Other causes of earthquakes include volcanism, artificial induction, reservoir induction, and nuclear explosions.

Earthquakes have varied effects including changes in geologic features, damages to man-made structures, and impact on human and animal life. Most of these effects occur on solid ground, but since most earthquake foci are actually located under the ocean bottom, severe effects are often observed along the margins of oceans, some of which are tsunamis.

1.1.1 Size of Earthquake

The size of an earthquake is an indirect measure of the quantity of energy released at the earthquake focus. Over the years, attempts have been made to describe the size of individual earthquakes. Before measuring instruments were invented, intensity scales were used. Major intensity scales include the Mercalli Scales and the Modified Mercalli Scales; these were based on the description of an earthquake in terms of its effect on structures and environment. After the invention of measuring instruments, different magnitude scales were developed. Examples are Body wave Magnitude (M_b), Surface wave Magnitude (Ms), Richter’s (local) Magnitude (M_L), and Moment Magnitude (M_w).

1.2 Seismic Activity

Seismic activity (also known as seismicity) is the study of the worldwide distribution of earthquake sources over a period of time. It also refers to the frequency, type and size of earthquakes experienced over a period of time. Earthquake sources are not uniformly distributed throughout the world, but concentrate along certain narrow regions in between the lithospheric plates. The major world seismic zones are the circum-pacific zone, which produces 75 - 80 % of the annual events and the Mediterranean, Transasiatic/Alphine zone which is responsible for about 15 – 20% of the global events. This zone extends from Indonesia through the Himalayas to the Mediterranean. Oceanic ridges also contribute in minute proportion (about 3-7%) of the global events (Lowrie, 1997). Mid-oceanic ridges are centres of ocean floor spreading which is a notable phenomenon that enhances the motion of the lithospheric plates. The remaining part of the earth is said to be aseismic (i.e. not seismically active). But no portion of earth is said to be free of earthquakes because there are intraplate earthquakes.

A common tool in seismicity study is Gutenberg-Richter (G-R) Frequency-Magnitude relation (Gutenberg and Richter, 1942) that is given by

$$\mathrm{Log}_{10} N = a - bM \tag{1.1}$$

Where N is the number of events for a known period of time; M is magnitude; a represents vertical intercept which indicates the total seismicity rate of the region and b is a tectonic parameter describing the relative abundance of large to smaller shocks

The G-R relation is an empirical formula which describes the distribution of global seismicity in terms of number of earthquakes of various magnitudes over a period of time. In its original form, it was based on the seismicity of the whole Earth. Thereafter, the formula has been used for studying the seismicity of different regions of the earth e.g. (Aki, 1965; Jolly and McNutt, 1999).

1.3 Justification for the Research

The G-R formula cannot be used for rating seismic activities of two or more regions because of the following limitations:

1. It does not contain information about the geographical area covered by the epicenters of earthquakes; hence, a small region that is very active could have smaller value of a than a large region that is just moderately active.
2. The constant a is a count of the total number, N, of events of different magnitudes combined together, without considering the effect of the energy generated by different magnitudes. This is equivalent to adding unlike terms since the energy due to magnitude m earthquake is proportional to 10^m.

3. The use of the G-R relation assumes that both constants a and b are defined. However, occurrence of earthquakes with close magnitude range within a region of interest yield indeterminate constants a and b since G-R curve will be almost parallel to the vertical axis.

In view of these three limitations the G-R relation is insufficient for rating seismic activities of regions without ambiguity. The development of methods for reliable rating of seismic activities is the main focus of this research work.

1.4 Aims and Objectives

The aims and objectives of this work were:

1. To develop models for rating seismic activities which take care of the limitations of the G-R method.
2. To use the models to rate seismic activities of selected regions in the world seismic zones.

1.5 Outline of the Thesis

Chapter 1 presents a brief introduction to the background of the research and problem of the research.

Chapter 2 presents the relevant background information in the following order:

- classification of various magnitude scales used in measuring earthquakes,
- approaches for representing G-R constants a and b values
- conventional methods for application of G-R constants a and b values.

Chapter 3 presents the methodology of developing the models for categorizing seismic activities when G-R constants a and b values are defined and also when G-R constants a and b values are not defined. The application of the two models developed on 10 regions in the world seismic zones using Fifty-year (1956 - 2005) earthquake data obtained from the Catalogue of Advanced National Seismic System (ANSS), U.S.A. to generate results towards categorizing seismic activities of each region without ambiguity.

Chapter 4 presents comprehensive evaluation of results for both models applied.

Chapter 5 presents the conclusion. This is followed by the list of references and appendix.

CHAPTER TWO

LITERATURE REVIEW

2.1 Theory of Earthquakes

An earthquake is a phenomenon that results from a sudden release of stored energy in a confined region of the Earth interior, resulting into the propagation of mechanical waves known as seismic waves. At the Earth's surface, earthquakes may manifest themselves by a shaking or displacement of the ground and sometimes tsunamis, which may lead to loss of lives and destruction of property.

Earthquakes may occur naturally or as a result of human activities. In its most generic sense, the word earthquake is used to describe any seismic event-whether a natural phenomenon or an event caused by humans-that generates seismic waves.

Most naturally occurring earthquakes are related to the tectonic nature of the Earth. Such earthquakes are called tectonic earthquakes. The Earth's lithosphere is a patch work of plates in slow but constant motion caused by the heat in the Earth's mantle and core. Plate boundaries glide past each other, creating frictional stress. When the frictional stress exceeds a critical value, called local strength, a sudden failure occurs. The boundary of tectonic plates along which failure occurs is called the fault plane. When the failure at the fault plane results in a violent displacement of the Earth's crust, the elastic strain energy is released and elastic waves are radiated, thus causing an earthquake. It is estimated that only 10 percent or less of an earthquake's total energy is ultimately radiated as seismic energy, while most of the earthquake's energy is used to power the earthquake fracture growth and is eventually converted into heat. Therefore, earthquakes lower the Earth's available potential energy and thermal energy, though these losses are negligible. To describe the physical process of occurrence of an earthquake, seismologists use the Elastic-rebound theory.

The majority of tectonic earthquakes originate at depths not exceeding a few tens of kilometers. Earthquakes occurring at boundaries of tectonic plates are called interplate earthquakes, while the less frequent events that occur in the interior of the lithospheric plates are called intraplate earthquakes.

Where the crust is thicker and colder, earthquakes occur at greater depths of hundreds of kilometers along subduction zones where plates descend into the Earth's mantle. These types of earthquakes are called deep focus earthquakes. They are possibly generated when subducted lithospheric material catastrophically undergoes a phase transition (e.g., olivine to spinel), releasing stored energy—such as elastic strain, chemical energy or gravitational energy—that cannot be supported at the pressures and temperatures present at such depths. Earthquakes may also occur in volcanic regions and are caused by the movement of magma in volcanoes. Such quakes can be an early warning of volcanic eruptions.

A recently proposed theory suggests that some earthquakes may occur in a sort of earthquake storm, where one earthquake will trigger a series of earthquakes each triggered by the previous shifts on the fault lines, similar to aftershocks, but occurring years later, and with some of the later earthquakes as damaging as the early ones. Such a pattern was observed in the sequence of about a dozen earthquakes that struck the Anatolian Fault in Turkey in the 20th Century, the half dozen large earthquakes in New Madrid in 1811-1812, and has been inferred for older anomalous clusters of large earthquakes in the Middle East and in the Mojave Desert (Jennings, 1985)

Most of large earthquakes are accompanied by smaller ones that can occur either before or after the main shock; these are called foreshocks and aftershocks, respectively. Aftershocks can be felt from half way round the world, for instance aftershock from New Zealand could be felt in England. While almost all earthquakes have aftershocks, foreshocks occur in only about 10% of events. The power of an earthquake is always distributed over a significant area, but in large earthquakes, it can even spread over the entire planet. Ground motions caused by very distant earthquakes are called teleseisms. The Rayleigh waves from the Sumatra-Andaman Earthquake of 2004 caused ground motion of over 1 cm even at seismometers that were located far from it (Lay and Kanamori, 2005). Using such ground motion records from around the world, seismologists can identify a point from which the earthquake's seismic waves apparently originated. That point is called its focus or hypocenter and usually coincides with the point where the fault slip started. The location on the surface directly above the hypocenter is known as the epicenter. The total length of the section of a fault that slips, the rupture zone, can be as long as 1,000 km for the biggest earthquakes.

Earthquakes that occur below sea level and have large vertical displacements can give rise to tsunamis, either as a direct result of the deformation of the sea bed due to the earthquake or as a result of submarine landslides directly or indirectly triggered by the quake. More than 3,000 perceptible earthquakes occur each year. Perhaps only 7 to 11 of these will involve significant loss of life, but the combined average annual death toll may exceed 10,000. In fact, the loss of life in extreme earthquakes may be more than ten times that caused by extreme volcanic eruptions. Such events may result not only in high death tolls, but also in overwhelming numbers of causalities requiring immediate medical treatment, and in serious long-term difficulties over housing and reconstruction. However, they seldom cause major problems of lack of food and drink and rarely result in large-scale population migrations.

Using a combination of instrumental monitoring and popular observation of natural phenomena the Chinese were able to predict the earthquake which devastated the city of Haicheng in Liaoning Province on 4 February 1976 (Adams, 1976). Prompt evacuation almost certainly saved many thousands of lives. However, the following year it proved impossible to predict the tremors which leveled Tanghan, a city of 1 million inhabitants, 230,000 of whom died in the catastrophe. More than a decade and a half later, the Haicheng prediction remains the only large-scale success of its kind, and routing forecasting of strong motions of the ground is unlikely to be achieved in the near future, although the Chinese do claim to have successfully predicted at least ten earthquakes, including some with magnitudes in the range 6.7-7.2 (Blundell, 1977).

Earthquakes occur most often along geologic faults, narrow zones where rock masses move relative to one another.The major fault lines of the world are located at the fringes of the huge tectonic plates that make up the Earth crust.

2.1.1 Induced Earthquakes

Some earthquakes have anthropogenic sources, such as extraction of minerals and fossil fuel from the Earth's crust, the removal or injection of fluids into the crust, reservoir-induced seismicity, massive explosions, and collapse of large buildings. Seismic events caused by human activity are referred to by the term induced seismicity. They however are not strictly earthquakes and usually show a different seismogram than earthquakes that occur naturally.

A few earthquakes have been associated with the build-up of large masses of water behind dams, such as the Kariba Dam in Zambia, Africa, and with the injection or extraction of fluids into the Earth's crust (e.g. at certain geothermal power plants and at the Rocky Mountain Arsenal). Such earthquakes occur because the strength of the Earth's crust can be modified by fluid pressure. Earthquakes have also been known to be caused by the removal of natural gas from subsurface deposits, for instance in the northern Netherlands. The world's largest reservoir-induced earthquake occurred on December 10, 1967 in the Koyna region of western Maharashtra in India. It had a magnitude of 6.3 on the Richter scale. However, the U.S. geological survey reported the magnitude of 6.8. (Bhatia et al., 2006)

The detonation of powerful explosives, such as nuclear explosions, can cause low-magnitude ground shaking. Thus, the 50-megaton nuclear bomb code-named Ivan detonated by the Soviet Union in 1961 created a seismic event comparable to a magnitude 7 earthquake, producing the seismic shock so powerful that it was measurable even on its third passage around the Earth (William et. al., 1989). In an effort to promote nuclear non-proliferation, the International Atomic Energy Agency uses the tools of seismology to detect illicit activities such as nuclear weapons tests. The nuclear nations routinely monitor each other's activities through networks of interconnected seismometers, which allow to precisely locating the source of an explosion.

Earthquakes occur on a daily basis around the world, most detected only by seismometers and causing no damage. Large earthquakes however can cause serious destruction and massive loss of life through a variety of agents of damage, including fault rupture, vibratory ground motion (shaking), inundation (tsunami, seiche, or dam failure), various kinds of permanent ground failure (liquefaction, landslides), and fire or a release of hazardous materials e.g gas leaks or petrol leaks. In a particular earthquake, any of these agents of damage can dominate, and historically each has caused major damage and great loss of life; nonetheless, for most earthquakes shaking is the dominant and most widespread cause of damage. There are four types of seismic waves that are all generated simultaneously and can be felt on the ground. Responsible for the shaking hazard, they are P-waves (primary waves), S-waves (secondary or shear waves) and two types of surfaces waves, (Love waves and Rayleigh waves).

2.1.2 Causes and Effects of Earthquakes

The energy released during an earthquake could be in the form of elastic strain energy, gravitational potential energy or chemical energy. Of all these, the release of elastic strain is the most important cause because this form of energy is the only kind that can be stored in sufficient quantity in the Earth to produce major disturbances. Earthquakes associated with this type of energy release are called tectonic earthquakes. Other causes of earthquakes include volcanism, artificial induction, reservoir induction, and nuclear explosions.

Earthquakes have varied effects including changes in geologic features, damages to man-made structures, and impact on human and animal life. Most of these effects occur on solid ground, but since most earthquake foci are actually located under the ocean bottom, severe effects are often observed along the margins of oceans, some of which are tsunamis.

2.1.3 Tectonic Earthquakes

Tectonic earthquakes are explained best by the elastic rebound theory. According to the theory, a tectonic earthquake occurs when strains in rock masses have accumulated to a point where the resulting stresses exceed the strength of the rocks and sudden fracturing results. The fracture propagates through the rocks. As a fault rupture progresses along or up the fault, rock masses are flung in opposite directions and thus spring back to a position where there is less strain. At any one point this movement may take place not at once but rather in irregular steps; these sudden slowings and restartings gives rise to the vibrations that propagate as seismic waves.The point where the fault rupture starts is the earthquake focus, while the point on the ground directly above the focus is called the epicenter. Tectonic earthquakes accounts for about 90% of global events.

2.2 Theory of Seismic Waves

The properties of any material are characterized by the elastic moduli or constants, which specify the relation between the stress and strain. A stress is measured as force per unit area and is compressive (or tensile) if it acts perpendicular to the area and shearing if it acts parallel to it. The strains in a body are deformations that produce restoring forces opposed to the stresses. Tensile and compressive stresses give rise to longitudinal and volume strains, which are measured as the change in depth per unit length or change in volume per unit volume. When the stress applied to an elastic medium is released suddenly the strain propagates within the medium as an elastic wave. When an earthquake or explosion occurs within the earth, part of the energy released is in form of elastic waves, which are transmitted through the rocks with definite velocity depending on the density and elastic moduli.

2.2.1 Types of Seismic Waves

There are two main types of seismic waves; body waves and surface waves.

2.2.2 Body waves

Body waves are waves that propagate through the body of the earth and obey the laws of geometrical optics, being reflected and refracted where the velocity changes.

There are two types of body waves.

a. **Compressional or primary** waves (p-waves): These are waves in which the vibrations are longitudinal to the direction of propagation. They travel faster and always the first to arrive at the seismographs. They do not cause any rotation in the medium and are called irrotational waves. The velocity of the p-waves is given by:

$$V_p = \sqrt{\frac{K + \frac{4}{3}\mu}{\rho}} \qquad 2.1$$

Where :

K = Bulk Modulus of the medium

μ = Rigidity of the medium

ρ = Density of the medium

These travel as elastic motion at the highest speeds.They are longitudinal waves that can be transmitted by both solid and liquid media in the Earth's interior.

b. **Shear or secondary waves (S-waves):** These are waves in which the vibrations are transverse or perpendicular to the direction of propagation. The propagation of S-waves causes rotation of material of the medium without changing it. They are rotational and equivoluminal waves. One notable propagation characteristics of S-waves is their inability to propagate through fluids since fluids have zero rigidity. The velocity of S-wave is given by:

$$V_s = \sqrt{\mu/\rho} \qquad 2.2$$

These are slower compared with P-waves and can only propagate through solid material.

2.2.3 Surface Waves

These are seismic waves that propagate through a region bounded by free surface of the Earth and the layer very close to the Earth's surface. These are waves which are guided along the surface of the earth and the layers near the surface. They do not penetrate into the deep interior. Surface waves are generated best by shallow earthquakes and arrive at the seismographs after the main P and S waves because their velocities are lower than those of the body waves. Surface waves are attenuated at a lower rate than body waves so they always have large amplitude on the seismogram. Also they travel longer distances than body waves. There are two types of surface waves:

(a) Rayleigh waves: These type seismic waves are caused by the superposition of P-waves and SV-waves (SV-waves are vertically polarized S-waves). They cause ground roll due to the fact that they cause the medium of propagation to undergo an elliptical motion which is retrograde to the direction of their propagation. Rayleigh waves are a type of surface wave that travel near the surface of solids. Rayleigh waves include both longitudinal and transverse motions that decrease exponentially in amplitude as distance from the surface increases. There is a phase difference between these component motions. The existence of Rayleigh waves was predicted in 1885 by Lord Rayleigh, after whom they were named. In isotropic solids these waves cause the surface particles to move in ellipses in planes normal to the surface and parallel to the direction of propagation – the major axis of the ellipse is vertical. At the surface and at shallow depths this motion is retrograde, that is the in-plane motion of a particle is counterclockwise when the wave travels from left to right. In addition, the motion amplitude decays and the eccentricity changes as the depth into the material increase. The depth of significant displacement in the solid is approximately equal to the acoustic wavelength. Rayleigh waves are distinct from other types of acoustic waves such as Love waves or Lamb waves, both being types of guided wave in a layer, or longitudinal and shear waves, that travel in the bulk. Rayleigh waves have a speed slightly less than shear waves by a factor dependent on the elastic constants of the material. The typical speed is of the order of 2–5 km/s. Surface waves therefore decay more slowly with distance than do bulk waves, which spread out in three dimensions from a point source. In seismology, Rayleigh waves (called "ground roll") are the most important type of surface wave, and can be produced, for example, by ocean waves, by explosions or by a sledgehammer impact. These are also called ground roll in exploration seismology. They are waves that propagate in the surface of a medium bounded by a free space or a vacuum. The particles in the wave front of the waves are vertically polarized and this gives rise to a resultant vertical motion that is elliptical in nature and the sense of motion is retrograde with respect to the direction of propagation. In an elastic solid medium where the Poisson ratio is non-zero, the speed of the Rayleigh wave V_{LR} is related to that of S-wave by

$$V_{LR} = \left(2 - {}^{2}\!/_{\sqrt{3}}\right)^{1/2} \beta \approx 0.92\beta \tag{2.3}$$

Their depth of penetration,d, in the Earth is related to their wavelength, λ, according to the equation :

$$d = 0.4\lambda \tag{2.4}$$

Therefore L_R waves undergo dispersion with depth. Since depth of penetration is proportional to wavelength, long periods LR waves contain more information about deep velocity structure of the earth while shorter periods LR waves contain information about shallow structure. Both vertical and horizontal seismographs can record LR waves.

(b) Love waves: Love waves occur where there is a general increase of S-wave velocity with depth. They result from of SH-waves (these are horizontally polarized S-waves) trapped between two material media near the Earth's surface and travel by multiple reflection of the SH-waves. The speed of their propagation is given by the inequality 1.5 below :

$$V_{S\min} \angle V_{LQ} \angle V_{S\max} \qquad 2.5$$

Where

V_{LQ} is the speed of love wave

V_{Smin} is the minimum speed of SH-waves

V_{Smax} is the maximum speed of SH-waves

The particle motion is transverse and horizontal. They are dispersive meaning that velocities depend on frequencies. i.e. different frequencies travel at different velocities. The first surface wave to arrive at the seismograph is of those frequencies that have the greatest velocity. LQ groups usually travel faster than LR so they are the first surface waves to arrive at the seismograph. These waves propagate in a medium where S-wave velocity increases with depth. The particle motion of a Love wave forms a horizontal line perpendicular to the direction of propagation (i.e. are transverse waves). Moving deeper into the material, motion can decrease to a "node" and then alternately increase and decrease as one examines deeper layers of particles. The amplitude, or maximum particle motion, often decreases rapidly with depth. Since Love waves travel on the Earth's surface, the strength (or amplitude) of the waves decrease exponentially with the depth of an earthquake. Surface waves therefore decay more slowly with distance than do body waves, which travel in three dimensions. Large earthquakes may generate Love waves that travel around the Earth several times before dissipating. Since they decay so slowly, Love waves are the most destructive outside the immediate area of the focus or epicentre of an earthquake. They are what most people feel directly during an earthquake.

2.3 Methods of Rating Individual Earthquakes

Over the years, attempts have been made to categorize individual earthquakes as they occurred. Earthquake intensities were used in the pre-instrumental era while magnitudes have been in use since invention of seismographs. The first systematic classification of earthquake intensity is probably that invented in the 1780s by Domenico Pignataro, an Italian physician. He reviewed all available accounts of 1,181 earthquakes and classified them as slight, moderate, strong and very strong. He denoted the Calabrian earthquakes of 1783, which killed at least 29,500 people, as "violent". At the same time a priest, Father Elisio della Concezione, produced the first known damage map (at a scale of 1:145, 600), in which he used astronomy to determine the co-ordinates of towns and a "star rating" to indicate the level of damage to each town or village (Alexander, 1993)

2.3.1 Earthquake Intensity Scales

A scale for rating individual earthquakes was proposed in 1828 by P.N.G. Egen. It contained six classes of intensity which were more sharply defined than those developed thereafter. The next advance was that of the Irish engineer Robert Mallet, who was one of the principal founders of modern seismology. Mallet combined theoretical and archival scholarship with a rigorous field investigation of southern Italy directly after the earthquake disaster of December 1857, which killed nearly 9,750 inhabitants of the Kingdom of Naples (Guidoboni & Ferrari 1987). His methods of recording earthquake damage were highly systematic and analytical, and new scales could thus be propounded on the basis of information that was much more comprehensive and less subjective than had previously been the case. However, the scales remained inductive, that is, they were derived directly from observed phenomena, with only limited input of explanatory of predictive theory.

The foundations of modern scales were laid in 1879 by De Rossi, an Italian, and were further developed in 1883 by Forel, a Swiss. Their scale of 10 classes was broadened to 12 by Giuseppe Mercalli, who in 1902 proposed what has proved to be the most durable system for classifying perceptible seismic phenomena. In 1931 the Mercalli-Wood –Neumann Scale was introduced in order to take account of the effect of earthquakes on motorized vehicles, tall buildings and other modern inventions that were not significant in Mercalli's time (Wood & Neumann 1931). The principal modern variants of Mercalli's original scale are the Modified Mercalli (MM) Scale of 1956 (Table 2.1), which is standard in the Americas, and the Mercalli-Cancani-Sieberg (MCS) Scale, which is used widely in Europe. Other scales include the Medvedev-Sponheuer-Karnik (MSK) Scale (Karnik et al.1984), the Japan Meteorological

Association (JMA) Scale (which has seven classes, rather than the 12 utilized in Western scales), and the GOST Scale, which is standard in the Commonwealth of Independent States (Bolt et al. 1990). Right from time the development of earthquake scale has been of great concern to seismologists. Domenico Pignataro in the late 18th century made the first attempt to grade the severity of earthquakes. His analysis classified earthquakes as very strong, strong, moderate or slight. In the mid 19th century Mallet came out with a list of earthquakes and plotted their estimated locations and hence produced the first map of the world seismicity. He also used a four–stage intensity to classify earthquakes damage and constructed the first isoseismal maps.

Ross and Forel developed Ross-Forel intensity in the late 19th century that was made up of ten stages describing the effects of increasing damage. The Rossi-Forel scale is one of the first scales designed to describe the effects of an earthquake, at a given place, on natural features, on industrial installations and on human beings. The intensity differs from the magnitude which is a quantity describing the strength of an earthquake. Due to its limitations, particularly in respect to the relation with ground acceleration, it has been replaced by the Modified Mercalli scale.

Wadati (1931) in an attempt to develop an earthquake scale, constructed a chart of maximum ground motion against distance for a number of earthquakes and noted that larger earthquakes produced larger amplitudes. Richter (1935) used Wadati's ideas and methods to construct the first earthquake magnitude scale, which is used to measure the size of an earthquake. Medvedev-Sponheuer-Karnik (MSK) scale came into being in Europe in 1964 and had stages just as the MM scale but with the difference in details (Lowrie, 1997).

In 1992 the European macroseismic scale (EMS) was introduced. The twelve-stage EMS was based on MSK scale and further considered how unprotected structures are to earthquake damage and give more explanation on the extent of damage to structures with different building standards.

Molchan et al (1999) used the frequency-magnitude relation to construct a multi-scale seismicity model for the main shock in seismic risk assessment. Their analysis revealed an understanding of seismicity at different space-time scales.

Table 2.1: The modified Mercalli scale

I	Instrumental	Detected only be seismographs
II	Feeble	Noticed only be sensitive people
III	Slight	Resembling vibrations caused by heavy traffic
IV	Moderate	Felt by people walking; rocking of free standing objects
V	Rather strong	Sleepers awakened and bells ring
VI	Strong	Trees sway, some damage from overturning and falling objects.
VII	Very strong	General alarm, cracking of walls
VIII	Destructive	Chimneys fall and there is some damage to buildings
IX	Ruinous	Ground begins to crack and many, houses begin to collapse and pipes break
X	Disastrous	Ground badly cracked and many buildings are destroyed. There are some landslides.
XI	Very disastrous	Few buildings remain standing; bridges and railways destroyed; water, gas electricity and telephones out of action.
XII	Catastrophic	Total destruction; objects are thrown into the air, much heaving, shaking and distortion of the ground.

2.4 Earthquake Magnitudes

This is the experimentally measured amplitude of ground motion produced by a seismic wave. They are determined directly from seismograms and are related indirectly to the energy released during an earthquake.

Magnitude scales have a general relationship of the form :

$$M = Log(A/T) + F(h,\Delta) + C \qquad 2.6$$

(Dowrick, 1977)

Where,

A is the amplitude of the signal,

T is the dominant period,

F is a correction for the the variation of amplitude with earthquake depth,h, and distance, Δ, from the seismometer

C is the regional scale factor.

The early estimate of earthquake size was based on non-instrumental measures of the earthquake effects. Values such as the number of fatalities or injuries, the maximum value of shaking intensity, or the intense shaking were used as determinants of earthquake size. The problem with these kinds of measurement is that they don't have a good correlation. The damage and destruction produced by earthquake will depend on its location, depth, and nearness to populated regions and its 'true' size.

With the invention of seismometers it is now easy to accurately locate earthquakes and measure the ground motion produced by seismic waves. One of the means of quantifying earthquakes using seismogram is the magnitude.

Also the USGS defined magnitude as a logarithmic measure of the 'size' of an earthquake, which is related to the energy releases as seismic waves at the focus of an earthquake. As measures of earthquake size, magnitudes have two principal advantages. First, they are directly measured from seismogram without sophisticated signal processing. Secondly they yield units of 1, which are intuitively attractive: magnitude 5 earthquakes are moderate, magnitude 6 is strong, 7 are major, and 8 are great (Stein and Wysession, 2003).

Several factors influence the determination of earthquake magnitude. They include focal depth, distance between earthquake focus and observation station, frequency content of the sampled energy and earthquake radiation pattern.

Magnitudes are usually measured from the amplitude and period of seismic signals as they arrive and are recorded at a seismic station. For a given earthquake, the amplitude decreases with an increasing distance (due to geometric spreading and attenuation of signals) and a distance dependent correction is applied when computing magnitude to result in one value for each station. Although the magnitude scale has neither 'top' nor 'bottom' values, the highest magnitude ever known is about 9.5 and the lowest about -3.0 (USGS, 2000).

2.4.1 Richter's magnitude scale (M_L)

The first seismic magnitude scale was developed by Charles Richter in the early 1930's and was motivated by his desire to design the first catalogue of Southern California earthquakes. This catalogue contained several hundred events, whose size ranged from barely perceptible to large, and Richter felt than an earthquake description must include some objective measurement of size to assess its importance. Richter observed that the ground motion recorded by the seismometer, one could assign relative size to earthquakes. All of Richter's observations were made from data recorded on one type seismometer called Wood-Anderson seismometer at a distance of 100km from the epicenter. To permit calculation of magnitudes from Wood-Anderson seismogram (free period To=0.8sec, damping constant h=0.8, static magnification Vo = 2800) recorded at other distances, Richter introduced the concept of the 'zero magnitude earthquake' and worked out the relationship between its amplitude and epicentral distance empirically as given by (Eaton, 1992):

$$M_L = \log A\,(D) - \log A_o\,(D) \qquad 2.7$$

Where

A is the amplitude recorded

A_o is the amplitude of the zero magnitude earthquakes at epicentral distance D.

This magnitude scale is called the Richter magnitude or M_L for local magnitude. From the table of values of A_o (D), an approximate empirical formula has been derived:

$$M_L = \log_{10} A + 2.56 \log_{10} D - 1.67 \qquad 2.8$$

Where A is the displacement amplitude in 10-6 m and D is in kilometers. The formula is valid for 10 < D < 600km. For the Wood-Anderson torsion instrument the largest amplitude generally comes from the S-arrival. Individual estimates of M_L will exhibit some scatter due to directivity, radiation pattern, focusing and other effects (Shearer, 1999). However, a stable estimate can generally be obtained by taking the average results from different stations.

Local magnitude in its original form is rarely used today because Wood-Anderson instruments are not common, and of course most earthquakes do not occur in Southern California. However, M_L is still magnitude scale because it was the first widely used 'size measure' and all other magnitude scales are tied to it.

Secondly, many buildings have resonant frequencies near 1Hz, close to Wood-Anderson seismogram, so M_L is a good indication of the structural damaged an earthquake can cause.

Although the local or Richter magnitude is useful, the limitations imposed by instrument type and the distance range makes it impractical for determining size of earthquake recorded worldwide.

An approximate relationship exists between local magnitude and surface wave magnitude is as given by (Gutenberg and Richter, 1956).

$$M_s = 1.27\,(M_L - 1) - 0.016\,M_L^2 \qquad 2.9$$

and another one by Ambraseys and Boomer (1990) as:

$$0.80\,M_L - 0.60\,M_s = 1.04 \text{ or } M_s = 1.33\,M_L - 1.73 \qquad 2.10$$

The scale gives values similar to those given by the local magnitude scale; but because each is based on a measurement of one part of the seismogram, they do not measure the overall power of the source and can be negatively affected by saturation at higher magnitude values—meaning that they fail to report higher magnitude values for larger events. This problem sets in at around magnitude 6 for local magnitude; surface-wave magnitude saturates above 8. Despite the limitations of older magnitude scales, they are still in wide use, as they can be calculated rapidly, catalogues of them dating back many years are available, and the public is familiar with them.

2.4.2 Body wave magnitude (M_b)

This is a more general magnitude scale used for global seismology. It is defined as :

$$M_b = \text{Log}_{10}(A/T) + Q(h,\Delta) \qquad 2.11$$

Where

T is the dominant period of the measured waves

Q is the empirical function of range and depend that.

The body wave magnitude is related to surface wave magnitude (Geller, 1976) as follows:

$$M_b = M_s + 1.33 \qquad (M_s < 2.86) \qquad 2.12$$

$$M_b = 0.67\, M_s + 2.28 \qquad (2.86 < M_s < 4.90) \qquad 2.13$$

$$M_b = 0.33\, M_s + 3.91 \qquad (4.90 < M_s < 6.27) \qquad 2.14$$

$$M_b = 6.00 \qquad (M_s > 6.27) \qquad 2.15$$

The body wave magnitude is basically used to record earthquakes that occurred more than about 2000km away from the recording stations. It can be computed relatively fast because its value depends on the amplitude of the p-phase of an earthquake. P-phases are waves traveling through the body of the earth are interior and are first arrivals in a seismic station. For large earthquakes (magnitude greater than 6) M_b saturate i.e. if the actual size of the earthquake is larger, the value of M_b does not increase any more.

An equation proposed by Gutenberg in 19445 can be used to calculate a body-wave magnitude (M_b) from the maximum amplitude (A_p) of the ground motion associated with P-waves having a period of about 1-5s is given by:

$$Mb = \log\frac{(A_p)}{T} + 0.01\Delta^o + 5.9 \qquad 2.16$$

2.4.3 Surface wave magnitude (M_s)

It may be generally defined as :

$$M_s = Log_{10}(A/T) + 1.66Log_{10}\Delta + 3.3 \qquad 2.17$$

For Rayleigh wave measurements on vertical instruments. Since the strongest Rayleigh wave arrivals are generally at a period of 20s, the expression can be written as :

$$M_s = Log_{10}A_{20} + 1.66Log_{10}\Delta + 2.0 \qquad 2.18$$

It should be noted that the equation is applicable only to shallow events. Surface wave magnitude is also related to moments as given by Geller (1976) :

$$LogM_O = M_s + 18.89 \qquad (M_s<6.76) \qquad 2.19$$

$$LogM_O = 1.5\ M_s + 15.51 \qquad (6.76<M_s<8.12) \qquad 2.20$$

$$LogM_O = 3\ M_s + 3.33 \qquad (8.12<M_s<8.22) \qquad 2.21$$

$$LogM_O = 8.2 \qquad (M_s>8.22) \qquad 2.22$$

Beyond about 600km, the long period seismograms of shallow earthquakes are dominated by waves traveling along the surface. The waves often have a period of approximately 20 seconds and depth less than 50km (USGS). They travel slower than p-waves and hence take a long time before they arrive at a seismic station. The amplitude of these waves depends on the distance. The depth of the source affects the nature of the s3eismic wave train even when the same energy is released. An earthquake with deep focus generates only a small surface wave train while shallow earthquakes cause very strong surface waves. As a result these shallow earthquakes are more prone to cause damage than deep ones (Lowrie, 1997).

Since M_s is measured from 20s period waves "saturation "starts only for very large (magnitudes larger than 8) earthquakes. The slow surface wave speed is the reason why it is difficult to quickly differentiate between a strong and very strong (Magnitude > 6) earthquake.

However, both M_s and M_b were designed to be compatible with M_L and at times all the three magnitude scales give the same magnitude values. But because they use different information from the seismic wave from they do not always agree.

A commonly used equation for computing surface wave magnitude (M_s) of a shallow focus earthquake from seismograph records at epicentral distances greater than 20^o is the one proposed by Bath in 1966 as:

$$M_s = \log_{10} (As/T) + 1.66 \log_{10} \quad + 3.3\Delta \qquad 2.23$$

Where A is the ground motion amplitude in microns (μm) after the effects of the seismometers are removed, T is the wave period in seconds, and the distance Δ is in degrees. Since the strongest Rayleigh wave arrivals are generally at a period of 20s, this expression is often written as:

$$M_s = \quad \log_{10}A_{20} + 1.66 \log_{10} \quad + 2.0 \Delta \qquad 2.24$$

This equation holds for only shallow events. Surface wave magnitude is also related to moments as given by (Geller, 1976).

$$LogM_o = M_s + 18.89 \ (M_s < 6.76) \qquad 2.25$$

$$LogM_o = 1.5 M_s + 15.51 \ (6.76 < M_s < 8.12) \qquad 2.26$$

$$LogM_o = 3 M_o + 3.33 \ (8.12 < M_s < 8.22) \qquad 2.27$$

$$LogM_o = 8.2 \ (\log M_o > 28) \qquad 2.28$$

2.4.4 Moment magnitude (M_w)

Because of the limitations of the magnitude scales, a new, more uniformly applicable extension of them, known as **moment magnitude (M_w)**, was developed. In particular, for very large earthquakes moment magnitude gives the most reliable estimate of earthquake size. This is because seismic moment is derived from the concept of moment in physics and therefore provides clues to the physical size of an earthquake—the size of fault rupture and accompanying displacement and length of slippage—as of as well as the amount of energy released. So while seismic moment, too, is calculated from seismograms, it can also be obtained by working backwards from geologic estimates of the size of the fault rupture and displacement. The values of moments for different earthquakes range over several orders of magnitude, and because they are not influenced by variables such as local circumstances, the results obtained make it easy to objectively compare the sizes of different earthquakes. These characteristics, plus the seismic moment's immunity to saturation at higher magnitudes and compatibility with other magnitude scales, led Tom Hanks and Hiroo Kanamori to introduce in 1979 the moment magnitude (M_w) scale for representing the absolute size of earthquakes.

It is observed that M_b values begin to saturate at about $M_b = 5.5$ and M_s values at about $M_s = 8.25$, this motivated the development of moment magnitude, M_w ,by Kanamori (1977).

It is defined as :

$$M_w = \frac{2\log_{10} M_o}{3} - 10.7 \qquad 2.29$$

Where M_o is the moment measured in dyne-cm (10^5dyne = 1N; 10^7 dyne-cm = 1Nm).

The moment magnitude has an advantage of being related to a physical property of the source and it does not saturate for very large earthquakes.

Moment magnitude is the measure of total energy released by an earthquake. It is preferred to other magnitude scales because of its precision. Moment magnitude is not based on instrumental recordings of a quake, but on the area of the fault that ruptured in the quake. This means that the moment magnitude describes something physical about an earthquake. Mw is derived (based on theoretical considerations) from the seismic moment Mo, which is the product of the fault area times average displacement at the fault times material rigidity.

i.e.

$$M_o = \mu * \text{fault area} * \text{displacement}. \qquad 2.30$$

Where μ is the material rigidity.

To compare seismic moment with magnitude Mw, we use a formula developed by Kanamori in (1977) of the California Institute of seismology:

$$M_w = \tfrac{2}{3} \log M_o - 10.73 \qquad 2.31$$

$$\text{Log } M_o = 1.5\, M_w + 16.1 \qquad 2.32$$

Where the units of the moments are in dyne-cm. Since it is expressed in dyne-cm, it preserves the simplicity of the magnitude scale by giving values of order 1.0 compatible with other magnitude scales.

In theory, M_w does not saturate since M_o includes the complete earthquake rupture. Unlike other scales, the moment magnitude takes into consideration the geometrical relationships between the fault's orientation and the observers. M_w is approximately the same as M_s magnitude value.

2.4.5 Energy magnitude (M_e)

Energy released during an earthquake can be measurable directly from velocity from velocity seismograms and then converted to magnitude through the expression :

$$M_e = \frac{2}{3}\log_{10} E_S - 2.93 \qquad 2.33$$

Where $\text{Log}_{10}E_s$ and M_s are related through Richter's formula :

$$\log_{10} E_s = 4.8 + 1.5M_s \qquad 2.34$$

Where

E_s is the seismic energy in Joules.

From the above equations, energy magnitude can be given as :

$$M_e = 0.3 + M_s \qquad 2.35$$

According to the USGS, the total energy from an earthquake consists of energy needed to create new cracks in rock, energy expelled as heat through friction, and energy elastically radiated through the earth. Of all these, the only quantity that can be measured is that which is radiated through the earth. It is the radiated energy that shakes buildings and is recorded by seismographs.

The radiated energy can be measured in various ways. In the past the radiated energy was measured empirically (from observations) from magnitude Ms through the Richter's formula, $Log_{10}E_s = 4.8 + 1.5\ M_s$.

With modern instrumentation, energy can be measured directly from velocity seismograms and converted to magnitude. If E_s is the energy in joules, the energy magnitude M_e is obtained by:

$$M_e = (2/3)\log_{10} E_s - 2.93 \qquad 2.36$$

$$M_e = 0.3 + M_s \qquad 2.37$$

If M_e is not available, the seismic moment can provide an empirical estimate of radiated energy.

2.4.6 Fault Area Magnitudes (FA or MI)

This type of magnitude is compatible with an estimated M_b magnitude. It is commonly computed from the felt area for earthquakes, which occurred before seismic instruments were in general use. The estimates are based on isoseismal maps or defined areas using intensity-attenuation relationships.

2.4.7 Duration magnitudes (MD or CL)

These estimates are derived from the duration or coda length of earthquake vibrations. Duration or coda length magnitude scales are normally adjusted to agree with M_L estimates. The MD formulas vary for different geographic regions and for different seismographic instruments.

2.4.8 Local Magnitude Scale (M_L)

In 1930, Charles Richter introduced what is now called the local magnitude, M_L. This was determined by measuring the largest amplitude, A, recorded on a standard instrument, the Wood-Anderson seismograph. He noticed that plots of LogA versus range for different earthquakes generally exhibited a similar decay rate. This suggested that a range-independent measure of earthquake size could be provided by the offset in LogA from a reference event at the same range.

$$M_L = Log_{10}A(\Delta) - Log_{10}A_0(\Delta) \tag{2.38}$$

Where

A_0 is the amplitude of the reference event,

Δ is the epicentral distance.

(Shearer,1999)

A relationship between intensity and magnitude was developed by Gutenberg and Richter,(1956) and is given as :

$$M_L = (2/3)I_0 + 1 \tag{2.39}$$

Where I_0 is the highest intensity of the earthquake.

However, a relationship was established by Ambraseys and Boomer(1990) as :

$$M_s = 1.33M_L - 1.73 \tag{2.40}$$

Where M_s is the surface wave magnitude.

2.5 Global Seismicity

The earth's major earthquakes occur mainly in belts coinciding with the margins of tectonic plates (fig 2.1). This have long been apparent from early catalogs of felt earthquakes and is even more readily discernable in mordern seismicity maps, which show instrumentally determined epicenters. The most important earthquake belt is the circum-Pacific belt, which affects many populated castal regions around the Pacific ocean – as for example, those of New zealand, New Guinea, Japan, the Aleutian Islands, Alaska, and the western coasts of North and south America.

It is estimated that 80 percent of the energy presently released in earthquakes comes from those whose epicenters are in this belt. The seismic activity is by no means uniform throughout the belt, and there are a number of branches at various points. Because at many places the circum-Pacific belt is associated with volcanic activity it has been popularly dubbed the "Pacific Ring of Fire".

A second belt, known as the Alpine belt, passes through the Mediterranean region eastward through Asia and joins the cicum-Pacific belt in the East Indies. The energy released in earthquakes from this belt is about 15 percent of the world's total. There are also striking connected belts of seismic activity, mainly along oceanic ridges – including those in the Arctic Ocean and along the rift valleys of East Africa.

This global seismicity distribution is best understood in terms of its plate tectonic setting. An earthquake occurs when there is a sudden release of energy within a confined region of the earth. This may be due to elastic strain energy, kinetic energy, gravitational potential energy or chemical energy. Earthquakes resulting from the release of elastic energy are known as tectonic earthquakes. They constitute about 90% of the global events while those resulting from volcanic activities are known as volcanic earthquake. These are relatively small both in size and in number.

Earthquakes are also classified based on their focal depths. Earthquakes with focal depths less than 70km are called shallow earthquakes (fig 2.2a). They occur in all the seismically active zones and constitute 70% of global events. Shallow earthquakes occur only in the oceanic ridges. Intermediate earthquake have focal depth of 70-300km (fig 2.2b) and account for 12% of the global events and deep earthquakes have focal depth (fig 2.2c) greater than 300km (Lowrie, 1997). Both intermediate and deep earthquakes occur in the circum-pacific and Mediterranean-Transasiatic/Alphine zones and follow the process of plate subduction (fig 2.2d). Though there is a debate on the physical mechanism of deep earthquakes, H. Turner located some earthquakes at a significant depth. But his analyses were not accepted since he also located some events in the air above the surface. According to Shearer (1999), deep earthquakes are observed along dipping planes of seismicity called the Wadati-Benioff zones that extend to almost 700km depth.

A recent explanation of the strong patterns of seismically active belts surrounding largely aseismic areas is the plate tectonic theory. The theory describes the lithosphere of the earth as consisting of about seven large, and several smaller stable plates. The relative motions between adjacent plates give rise to earthquakes, mountain building, volcanism and other phenomena along the plate boundaries.

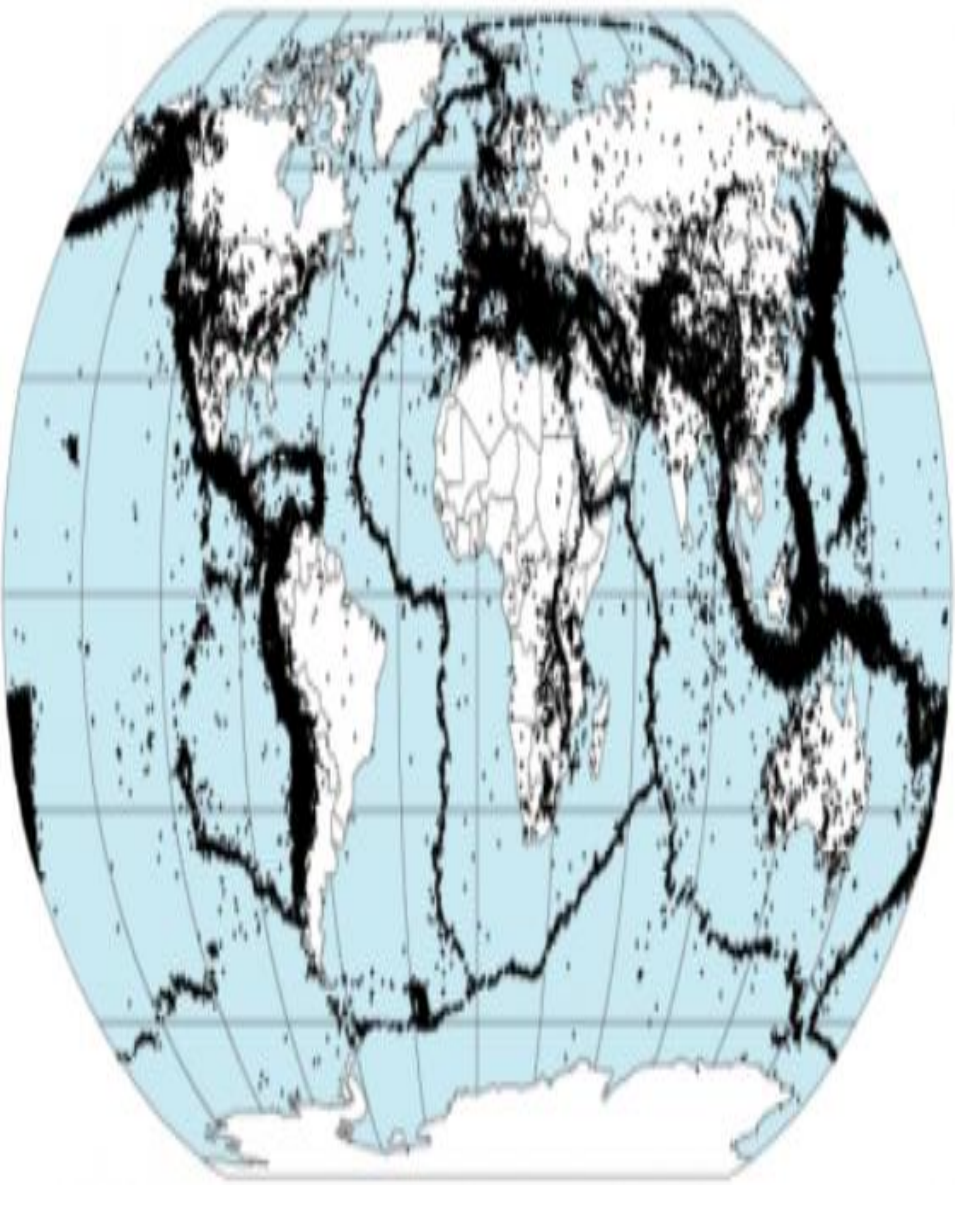

Fig. 2.1: Global Earthquake Epicentres (USGS, 2000).

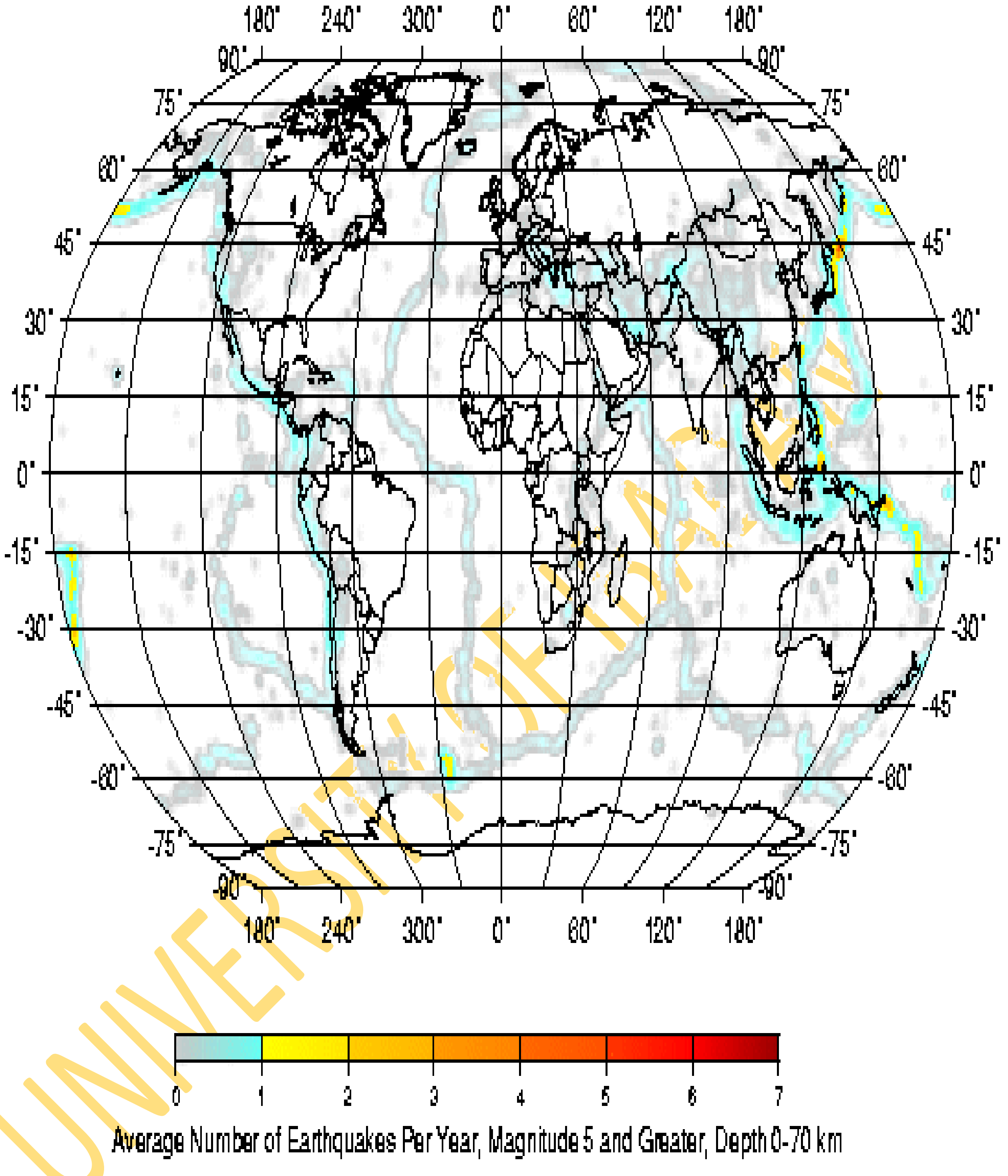

Figure 2.2a Global Shallow Earthquakes with Magnitude 5 and above (USGS, 2000).

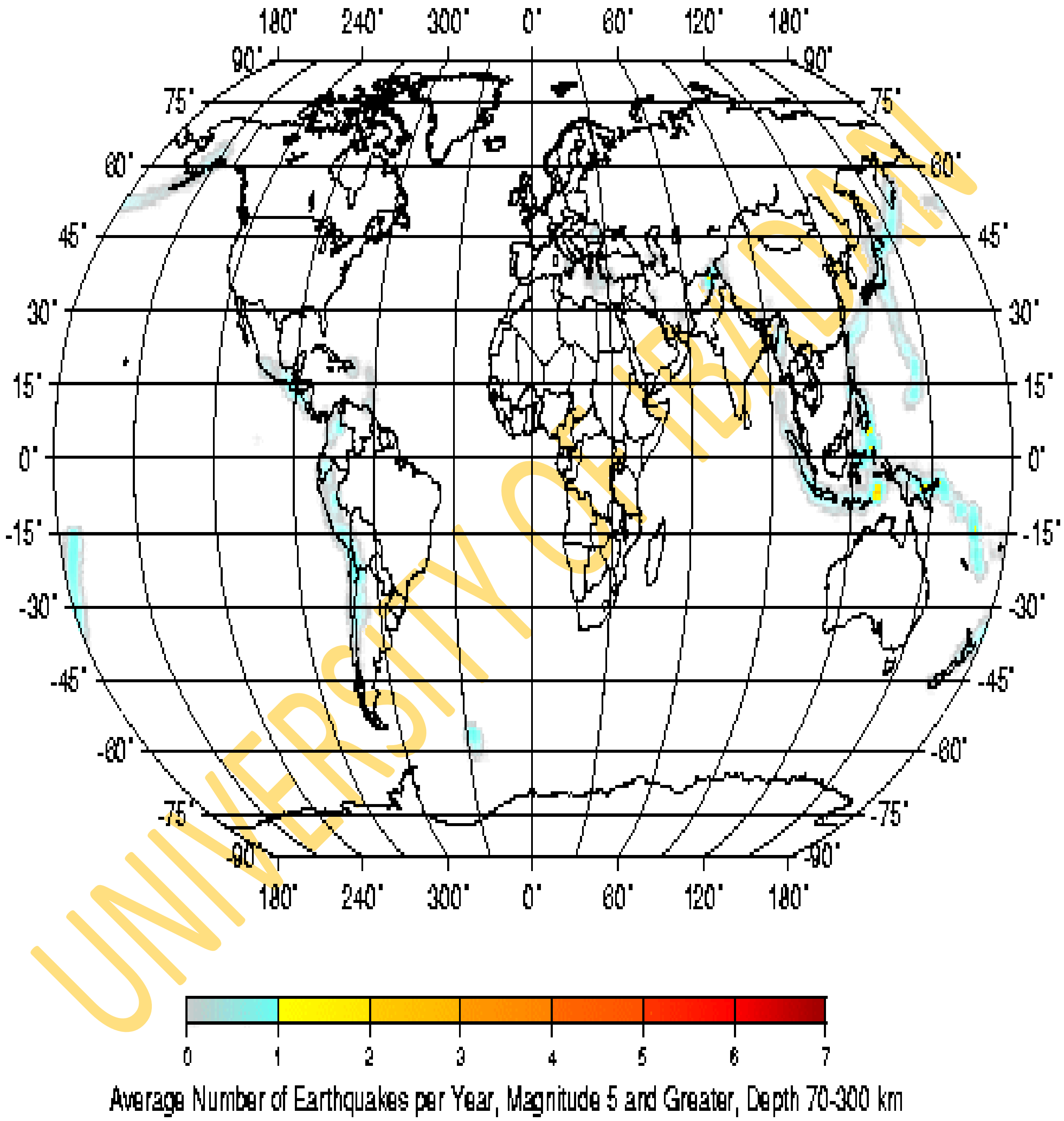

Figure 2.2b Global Intermediate Earthquakes with Magnitude 5 and above (USGS, 2000).

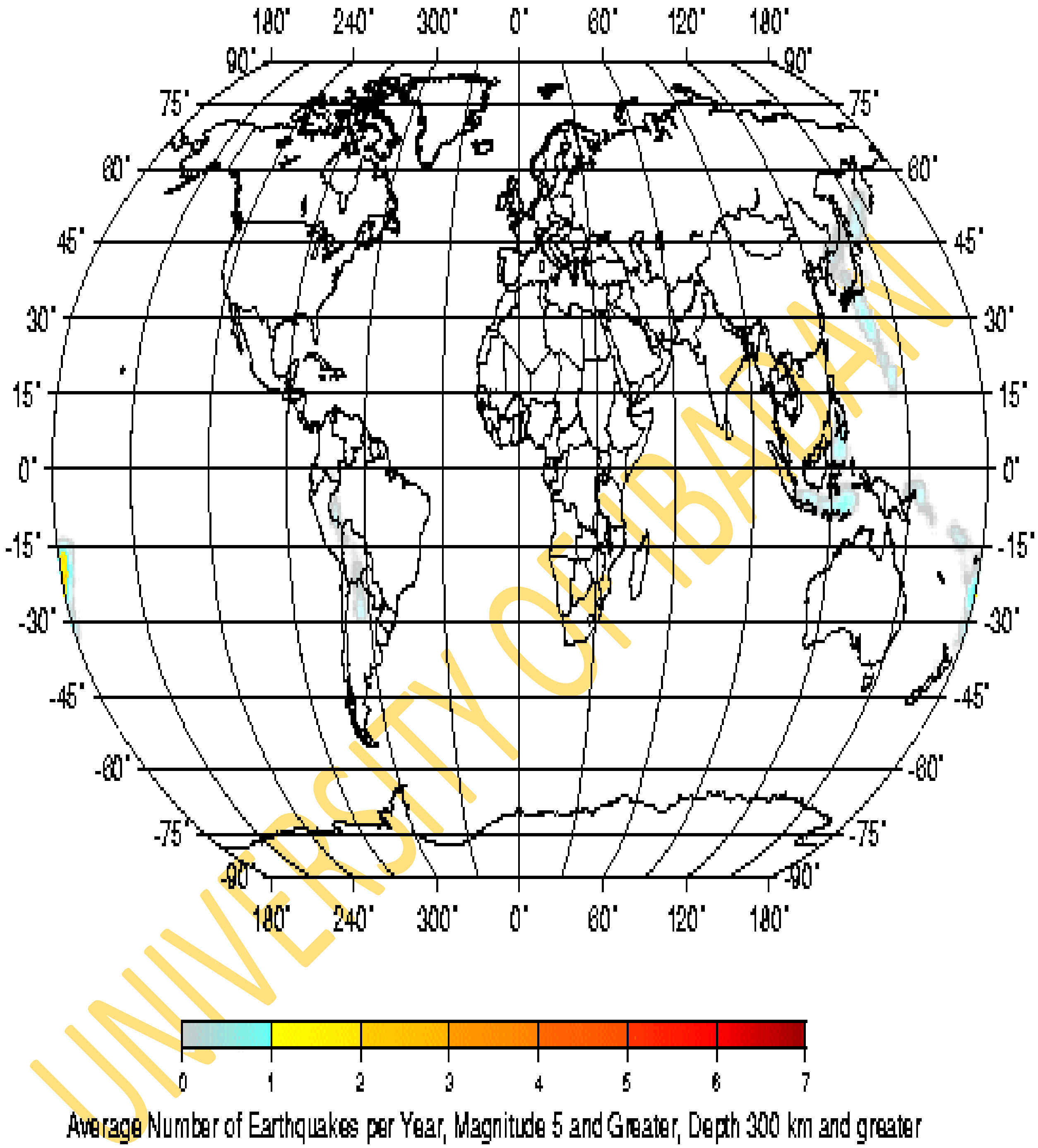

Figure 2.2c Global Deep Earthquakes with Magnitude 5 and above (USGS 2000).

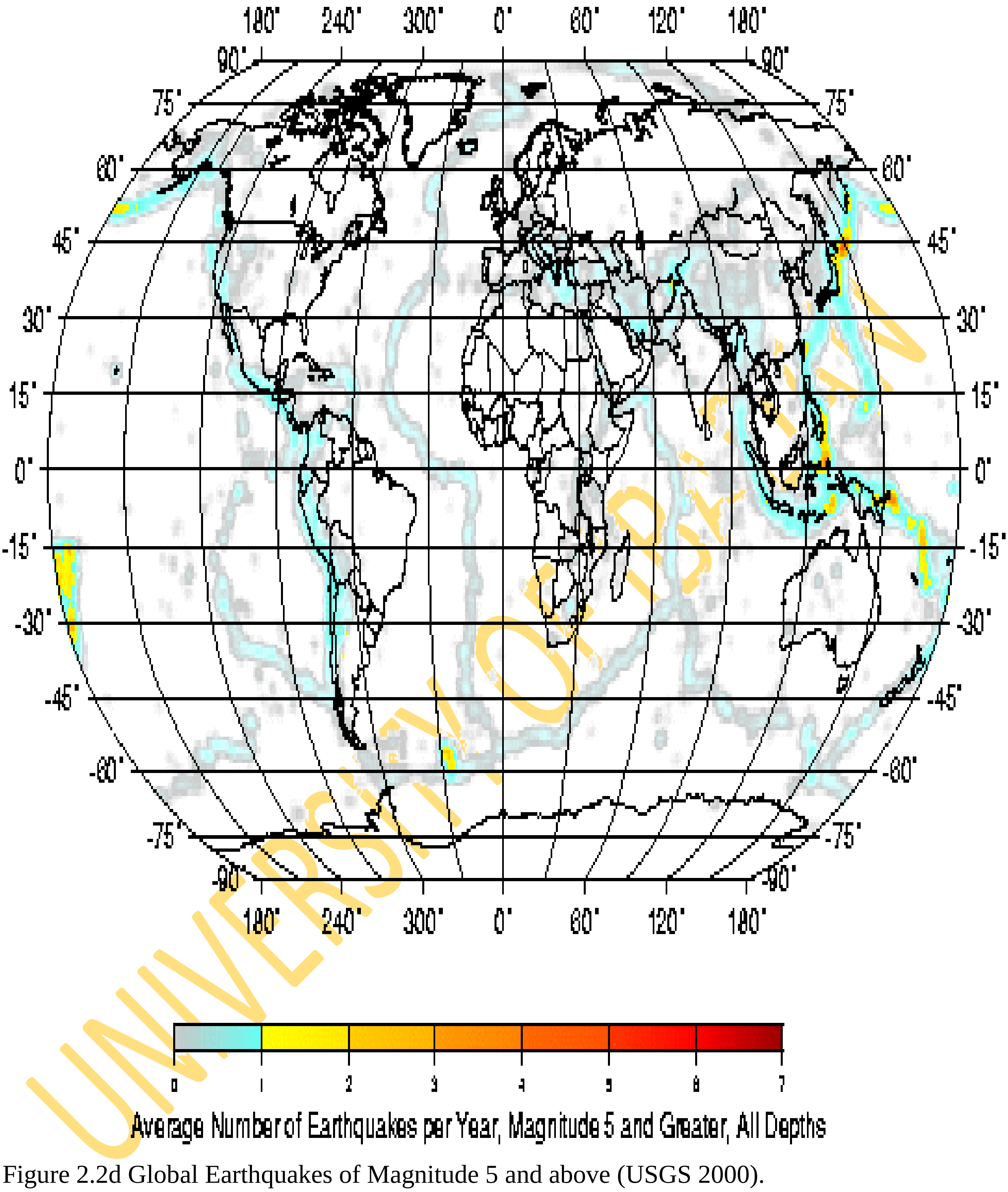

Figure 2.2d Global Earthquakes of Magnitude 5 and above (USGS 2000).

2.6 The Gutenberg – Richter Relation

Ishimoto and Iida first discovered the size distribution of earthquakes in a seismogenic volume in Japan in 1939 using the maximum trace amplitude of an earthquake. Later in 1944 Gutenberg and Richter established the magnitude frequency relationship. Their aim was to improve the estimation of the frequency of destructive earthquakes in California by mans of statistical method rather than rely on historical records alone. Their original formula Log N = a +b (8 –M) relates the frequency of earthquakes to the magnitude using the local magnitude M_1 as a magnitude scale. The more general non-cumulative form of the Gutenberg-Richter's relationship, that was employed this study is given by

$$\text{Log } N(M) = a - bM \qquad 2.41$$

Where N=number of earthquakes of magnitude $\geq$ **M** that occurred in the region over a period of time. **a** and **b** are regression constants **a** is a constant representing the total number of earthquakes with magnitude > 0 and is dependent on the location and time of the sample used. It also describes the level of seismicity in a given region **b** is the proportion of earthquakes of small and large magnitudes. The slope of the graph determines b. A steep slope corresponds to a high b-value, when the slope flattens; the b- value is getting lower.

Utsu (1965) proposed that b is given by:

$$b = \frac{\log e}{M - M_{\min}} = \frac{0.4343}{M - M_{\min}} \qquad 2.42$$

Which Aki (1965) identified as equivalent to the maximum likelihood estimate for **b.**

From Equation 2.41 it is observed that the number of earthquakes decreases logarithmically with the increase in the magnitude.

The nature of the earthquake frequency – magnitude distribution is of fundamental importance in probabilistic seismic hazard calculation and accordingly has attracted a great deal of concern. However, there are some arguments in favour of the quadratic form of Gutenberg-Richter's relationship because it is the most common. The log-linear relationship works well in the certain magnitude range and fails at the smallest magnitudes because the recording instruments under record small magnitudes. The relationship also fails at high magnitudes because maximum magnitude is achievable. Maximum magnitude arises because all traditional magnitude scales saturate i.e. they do not go beyond a certain value of magnitude. Secondly, a given fault or tectonic region has physical constraints on the maximum size of the event it can generate (Dowrick, 1977).

From the seminar on **b**-value by Kulhanek (2005), the G-R relation (Equation. 2.41), applies to cummulative number N as well as to incremental numbers,n. In other words, N is the cummulative number of earthquakes with magnitudes larger than M, while n is the number of events with magnitudes in the range $M \pm \Delta M$ (increamental or interval distribution). A choice of proper ΔM is a crucial task in any incremental **b** evaluation. However, cummulative distribution provides a better fit since numbers are larger and less degreded by statistics of small numbers. It also avoid the problem of designing a proper ΔM. Once a and b are determined, for a given region and time window, then one already has the information necessary to access parameters of seismic hazard. It should however be noted that the relation should not be expected to extrapolate without limits, the frequency of the smaller events to determine the threat of the rare large earthquakes.

2.7 Explanations of b-Value

Spatial and temporal variations of the **b**-value have earlier been employed in numerous seismicity studies. After pioneering works of Mogi (1962), Scholz (1968) and Wyss (1973), they have been extensively used (with varying degree of success) by other scientists e.g. to identify volumes of active magma bodies (Wiemer and Benoit, 1996; Wiemer et al., 1998), roots of regional volcanism (Monterroso and Kulhanek, 2003) and to forecast major tectonic earthquakes (Monterroso, 2003; Nuanin et al., 2005).

According to Kulhanek (2005), the linear relation holds only for magnitudes in the certain range $M_1 \leq M \leq M_2$. For small and large magnitudes, the frequency decreases more rapidly than linearly and consequently a non-linear fit may in some cases be a better approximation of observed data. He stated two explanations for the deviations from linearity as :

(i) At small magnitudes, there is incompleteness of data owing to under-recording of small events. Recent studies suggest that the decrease of **b** is just an artifact of catalog incompleteness but that small earthquakes are really not as numerous as a constant **b**-value extrapolated from larger events would predict. And so the decline in frequency may to a certain extent be real.

(ii) The saturation of magnitude scales at large magnitudes. Another is the length of available catalogs. To address this problem, the seismic moment, M_0, or the moment magnitude, M_w is used.

A significant increase in **b** is observed around M = 7.3 or around $M_0 = 10^{20}$ Nm (Pacheo et al., 1992) is interpreted as expressing the simultaneous saturation of fault dimension, W, and the slip, D, on the fault. But if the rate at which earthquakes occur is compared with predicted rates by plate rates, it will be too small.

Kulhanek (2005) concluded that plate motion does not take place on the earthquake faults. From some works e.g. Kagan (1999), it is advocated that **b** is essentially constant, but others e.g. Kulhanek, (1997); Wiemer et al., (1998); Gerstenbergeret et al., (2001), argue that spatial and temporal variations in **b** exist. Some of the observed scatter are :

$1.0 \leq \mathbf{b} \leq 1.6$	Mogi, global seismicity, $\mathbf{b}$~1.0 for lat. $\geq 40^0$, whereas $\mathbf{b}$~1.6 for lat. $\leq 40^0$
$0.3 \leq \mathbf{b} \leq 1.8$	Hurtig and Stiller (1984), global seimicity
$0.6 \leq \mathbf{b} \leq 1.5$	Udias and Mezcua (1997), global siesmicity
$0.8 \leq \mathbf{b} \leq 1.2$	McGarr (1989), global seismicity
$0.5 \leq \mathbf{b} \leq 1.5$	McGarr (1984), mining tremors (South Africa) and tectonic earthquakes
$0.6 \leq \mathbf{b} \leq 1.6$	Monterroso and Kulhanek (2003), central America seismicity
$0.6 \leq \mathbf{b} \leq 2.6$	Nuannin et al., (2002), mining tremors, Zinkgruvan, Sweden

2.7.1 Applications of b-Value

High and low stresses : According to the works of Scholz, (1968) and Wyss, (1973), high and low stresses cause earthquakes series with low and high **b**-values respectively. This is employed in the works of Wiemer and Benoit, (1996); Wiemer et al., (1998), to predict earthquakes and identify volumes of magma bodies.

Material heterogeniety : It is shown from the work of Mogi, (1962), that large heterogeneities in sub-surface materials correspond to higher **b**-values.

Thermal gradient : The work of Warren and Latham, (1970), showed that an increase of thermal gradient caused an increase of **b**-values from 1.2 to 2.7.

Aftershocks and foreshocks : From the works of Suyehiro et al.,(1964), it is found that aftershocks have large **b**-value while foreshocks have low **b**-value.

Swarms : Large departures from **b**~1 is shown in swarms sometimes as large as **b** =2.5. Swarms, by definition, lack a clear main shock and result from processes such as migration of magmatic fluids or caldera development.

Variation with depth : It has been observed that **b** varies laterally and with depth, low **b** implies shorter recurrence time. Patches with low **b** may be interpreted as possible stress concentrations reflecting variations in frictional properties along the fault, which may control the reccurence of the next large event.

Paleoseismic studies : There is a usual deviation of paleoseismic studies from the seismologically determined G-R relation. But the opposite is also observed, i.e. instrumental data show that large earthquakes ($M \geq 7.2$) are less frequent than expected from smaller events.

Small time-sampling : The **b**-value is reasonably well estimated from smaller earthquakes than for large ones.

Focal mechanism : Current research reveals that thrust fault events are associated with lower **b**-values compared with normal-fault events.

In the experiments of Mogi (1962), the effect of heterogeneity on **b**-value is demonstrated. The **b**-value and the fractal dimension, D, can be determined, following experiments involving acoustic emission by Main et al.,(1990). Temporal variations in D can be explained by fracture mechanics criteria for failure. The spatial variations of the **b**-values can be interpreted from both experiments and field observations of seismicity. It was shown that D=1 (**b** = 0.5) reflects critical stress concentration; with the probability of repeated fracture at a particular site at a maximum.

With D = 2 (**b** = 1), the probability is independent of previous events, corresponding to random process equivalent to background seismicity.

With D < 2 (**b** < 1), there is stress concentration leading to localisation of deformation with positive feed-back at low stress intensities such as dilatency, leading to highly diffuse fracture system.

In conclusion, fractal dimensions of flaws increases as stress intensities decrease because lenght distribution of cracks become more heterogeneous. However, conditions in the laboratory and in the field are obviously different in that the schizosphere is more heterogeneous than intact rock samples in the laboratory and **b** =1, D = 2 in the field, because the schizospere already contains major faults and stresses.

The effect of stress is demonstrated by experiments of Wiemer and Wyss (1997) where **b**-values decreased when ambient stress is increased in the laboratory. **b** is proportional to pore pressure in cases of fluid-induced seismicity; b decreases during mine burst; **b** is lower in compressive than in extensional tectonic regimes; and **b** increases with depth along strike-slip faults in California.

The effects of temperature shown by experiments of Wiemer and McNutt, 1998; Wyss et al., 1973, showed that there is an increase in **b**-value from regional values of **b** = 0.7 to values of **b** > 1.3 or even **b** = 1.5 in volcanic regions as we approach active magma chambers. This change in **b**-values can be explained if fractal dimension, D, is twice the b-value.

Conclusions obtained by Steacy et al., (1996), from a two-dimensional cellular automation with strength heterogeneity, but homogeneous tectonic loading was that the **b**-value increases with increasing range of fractal dimension of strength or roughness of the active fault zone.

The spatial mapping of **b**-value at Galeras volcano, Colombia, using earthquake data recorded from 1995 to 2002, a work carried out by Acevedo et al., (2005), involved the analysis of the catalog of volcano – tectonic earthquakes at Galeras volcano, Colombia, to determine the magnitude of completeness of seismograph network and also to explore the subsurface structure by mapping the **b**-value of the frequency-magnitude distribution. From observation of the two and three-dimensional mapping of **b**-value, a vertically elongated structure beneath the active active crater of Galeras down to a depth of 6km was illuminated. It could be associated with a conduit, or magma storage. This is the first discovery of its kind in previous studies of **b**-value on volcanoes around the world.

In the on-going **b**-value mapping of the Yellowstone volcanic and hydrothermal system by Farell et al. (2007), variations in **b**-values were observed and are been compared with existing crustal tomography results, to distinguish between causes which could be material heterogeneity, the applied shear stress, the effective stress and/or the thermal gradient of the area.

In the mapping of the **b**-value anomalies in Colfiorito tectonic zone (central Italy) and beneath Mt. Etna volcano (Sicily, Italy), a work by Murru et al. (2008), it was shown that spatial variations in **b**-

value observed was correlated to a process of lateral magma uprising, ending with a high velocity vertical dike emplacement which heralded to the 2001 lateral eruption.

In the work of Papazachos, (1999), Greece and the surrounding area was organised into a grid, the a and **b** values are simultaneously determined for the whole grid by solving an appropriate linear system. The results obtained were in good agreement with previous studies and further enhanced the knowledge of the study area.

Drakopoulous (1968) divided the region of Greece into many parts and obtained b for each case. His results showed that for almost all parts, values of b range between 0.4 and 1.7. One can therefore infer from this that b varies much more vertically than horizontally.

In addition, some authors have speculated that b-values may be influenced by thermal gradient causing the b-value to increase from 1.2 to 2.7 (Warren and Latham, 1970).

Minakami (1974) reported that A-type earthquakes (i.e. seismic events with clear P-waves and S-waves occurring beneath volcanoes) have b value of about 1.5 and for B-type earthquakes (i.e. seismic events occurring under volcanoes with emergent onset of P-waves, no distinct S-waves) b-values are higher than 2.0.

Some researchers are of the view that b-value varies from 0.5 to 1.0 for tectonic earthquakes and for volcanic events b-values are higher (Gresta and Patane, 1983).

Studies by Hurtig and Stiller (1984), Udias and Mezcua (1997) on global seismicity revealed that b-values range from 0.3 to 1.8, 0.8 to 1.2 and 0.6 to 1.5. McGarr (1984) on mining tremors (South Africa) and tectonic earthquakes revealed that b varies from 0.5 to 1.5 Agrawal (1991) confirmed this fact that tectonic earthquakes are characterized by the b-values from 0.5 to 1.5 and are more frequently at 1.0.

However, many researchers have investigated temporal changes of b. Most of these studies addressed bulk changes rather than temporal changes in sub volumes (Wiemer and Wyss, 2002). Some studies have investigated both spatial and temporal variability of b simultaneously (Ogata, 1991).

The rock burst in a mine and its related micro-seismicity (-2>M>0.5) before and after the mainshock was used by Urbancic et al. (1992) to investigate temporal and spatial changes in the b-value. They found that decreasing b-values correlate with increasing stress release estimates and that larger events tend to occur where the b-value has its steepest gradient. They further concluded that b-values “provide the best estimates for stress conditions within the seismogenic volume as they include information from both spectral – (seismic moment) and time domains ‘(peak amplitudes)’.

Holub (1996) investigated space-time variations of the frequency-energy relation for mining-induced seismicity in the4 Ostrava-Karvina mine district Czech Republic. He stated that lower b-values correspond to a higher level of induced seismic activity while high b-values correspond to a low and moderate seismic activity.

Systematic studies have been carried out by some researchers to examine the potential of temporal changes in b-value as a short-term, medium-term and long-term earthquake precursor. Results showed that large earthquakes are often preceded by a medium-term increase in b, followed by a decrease in the weeks-months before the earthquake (Sammonds et al., 1999). Molchan and Dmitrieve (1990) have studied temporal b-value variations for foreshocks during hours, days before the main shock. Molchan et al. (1999) found, from both regional and global earthquake catalogues, that the b-value of foreshocks drops by about 50%. From earthquake data for Central America from preliminary determination of epicenters (PDE) and E-catalogs Monterroso (2003) found evidence that supports the hypothesis that b-value decreases significantly prior to the occurrence of large earthquakes.

Wiemer and Wyss (1997) noted that the b-value in the Park field and Morgan Hill regions of California systematically decreases from high b>1.1 in the top 5km to b<0.8 below 6km depth.

Mori and Abercrombie (1997) confirmed this decrease with depth for several other regions in California and proposed that the lower b at depth corresponds to a higher probability of larger earthquakes to nucleate at depth. Though a decrease of b with depth has been firmly established for California, but the physical cause of this decrease is not yet established with certainty. Wiemer and Wyss (2002) have speculated that the change in ambient stress plays an important role.

Monterroso and Kulhanek (2003) investigated b-value variations with depth in the subduction zone of Central America. They observed high b-values in the upper part of the slab at depths around 80-110km beneath the volcanic chain in Guatemala-El Salvador. Nakaya (2004) analyzed seismicity data from the subducting slab along Kurile Trench. Results revealed a zone of anomalously low b-values near the hypocenter of the 26 September 2003, Tokachi-oki earthquake (M=8).

Though more facts have been established on spatial variation of b on a local region scale, arguments still exists about regional to global scale. Studies by Frohlich and Davies (1993) and Kagan (1999) reported that there is little variation of b between different tectonic regions and that the observed differences are at least partially as a result of artifacts rather than natural.

Moreover, the variation of b in subducting slabs has been studied. Wiemer and Benoit (1996) mapped well-defined anomalies similar to those found in the crust at a few kilometers beneath volcanoes at about 100km depths in the subduction zones of Alaska and New Zealand. They interpreted these anomalies as due to dehydration of the descending oceanic crust at top of the slab and proposed that their locations mark the origin of magma, feeding subduction zone volcanism.

Wiemer and Wyss (2002) reported that earthquake-size distribution in many tectonic regions on a local to regional scale reveal statistically significant variations in the range of at least 0.4 to 2.0 for the b-values in the frequency-magnitude distribution.

Also that explosion especially quarry blasts frequently contaminate seismicity data and this will cause bias in the b-estimates locally toward large values because on average, explosions are smaller than earthquakes.

They corroborated the fact that b-value underneath volcanoes is not, as initially thought to be, generally higher but that the pockets of anomalously high b-values are embedded in average crust. By comparing the anomalies of high values with other geophysical and geodetic data regarding the location and extend of magma chambers, they concluded that in the seismogenic surrounding of magma chambers high b-values are present and especially at shallow depths. The factors causing these high values were attributed to the presence of hot fluids in geothermal systems, or external cracking which a volume may have acquired during past eruptions. Hence high b-values give rise to high heterogeneity, high pore pressure and high thermal gradient. With regards to changes in b with time, they speculated that the fact that spatial variations of b on large scales have not been established could be as a result of lack of high quality earthquake catalogues with low magnitude of completeness on this scale; lack of rigorous studies or because heterogeneity in the earth exists mainly on smaller scales.

Enescu and Ito (2002) showed that b-values vary from 0.8 to 1.4. They discovered that areas that experienced larger slip during the main shock and during previous seismic activity have low stress because of more fracture and hence favour high b-values for the aftershocks. A large value of b in a give region or area shows a relative abundance in small earthquakes. Areas with low b-values on the other hand are probably under higher applied stress after the main shock. They also suggested that the rupture process in an earthquake and previous earthquake activity are the major factors controlling the spatial distribution of b-value.

Results on the investigation of the brittle ductile transition in rocks and associated seismicity (Amitrano, 2003) suggested that the b-value might be controlled by variation of the internal friction angle induced through changes in confining pressure/

Schorlemmer et al. (2004) have shown that b-value systematically varies from different styles of faulting. Normal faulting is associated with the higher b-values (about 1.1); strike-slip events show intermediate values (about 0.95) and thrust events the lowest values (about 0.75). It is possible b is related to focal mechanism (Kulhanek, 2005).

The findings of studies by Rao and Lakshmi (2005) on analysis of b- value of acoustic emissions accompanying rock fracture have revealed that while testing the material undergoing brittle failure b-value was found to range from 1.5 to 2.5 in the early stages. It later decreased with an increase in stress to attain values approximately 1.0 and less indicating temporal fluctuations as the impending failure approaches in the material. A high b-value was attributed to a large number of small acoustic events showing new crack growth. Whereas low b-values showed faster or unstable cracks growth accompanied by relatively high amplitude emission in large numbers.

Recent studies by Kullhanek (2005) has revealed that changes in b towards higher magnitudes may be due to the inability of the fault dimensions, especially width to keep growing indefinitely with the increasing earthquake size. He also suggested that the decrease of b-value (below threshold magnitude) is not just an artifact of catalogue incompleteness but that small earthquakes are not really as numerous as a constant b value extrapolated from large extents would predict and so decline in frequency may to a certain extent be real. His finding s also indicated that low b implies shorter recurrence time and patches with low b may be interpreted as possible asperities (i.e. stress concentration) reflecting variations in the fault which may control the recurrence of the next large events.

Lowrie (1997) stipulated that a-value varies from about 8 to 9 from one region to another. Study carried out by Wiemer and Wyss (2002a) in the frequency-magnitude for South California for years 1999-2000 showed that a-value is about 6.08. The higher the a-value in a given region the higher the seismicity (Paiboon Nuannin, 2006).

CHAPTER THREE

METHODOLOGY

3.1 Development of Models for Categorizing Seismic Activities

In this work, seismicity is described in terms of radiated energy of earthquakes. Considering an arbitrary region of area A where N earthquakes have occurred over a period T. For an earthquake of magnitude M, the radiated energy, E, is given by

$$Log_{10}E = 1.5M_w + 11.8 \qquad 3.1$$

Where M_w is the Moment Magnitude (Kanamori 1977)

From equation 3.1, the total energy radiated by an earthquake of magnitude M is given by:

$$E = 10^{(1.5M+11.8)} \qquad 3.2$$

The total energy per unit area per unit time for the whole period T was developed in terms of the following two models:

1. A model that does not involve the constants a and b at all. This takes care of situation where a and b may not be defined.
2. A model that involves a and b values for each of the sub-period s (where a and b are defined).

The two models were subject to the necessary condition that their rating of seismic activities for any set of selected regions must give a similar order and the order must be reasonable in terms of the observed radiated energy of earthquakes for the regions.

3.1.1 Model 1

Let the area of a region, G, be A. The radiated energy per unit area per unit time due to N earthquakes is defined as:

$$\Im_1 = \sum_i^N E_i \Big/ TA \qquad 3.3$$

Where E_i is the energy of the ith earthquake.

Substituting E in equation (3.3) yields,

$$\Im_1 = \sum_i^N \frac{10^{(1.5m_i + 11.8)}}{TA} \qquad 3.4$$

Where m = M_w

Let the area of a region G be A. Let the total time period T be divided into n equal subperiods, such that T can be written as

$$T = \sum_{i=1}^{n} s_i \qquad \text{(n is an integer)} \qquad 3.5$$

Let the number of earthquakes that occurred in G in subperiod s_i equal N_i. The amount of energy radiated per unit area per unit sub-period s_i in G is given by:

$$\overline{Es} = \sum_{l=1}^{N_i} \frac{E_l}{s_i A} \qquad 3.6$$

Substituting for E in equation 3.2, yields

$$\overline{E}_S = \sum_{l=1}^{N_i} \frac{10^{(1.5M_l + 11.8)}}{s_i A} \qquad 3.7$$

Hence, the total energy per unit area per unit time for G is given by:

$$\bar{E}_T = \sum_{i=1}^{n} \sum_{l=1}^{N_i} \frac{10^{(1.5M_l + 11.8)}}{s_i A} \qquad 3.8$$

$$\bar{E}_T = \sum_{i=1}^{n} \frac{1}{s_i} \sum_{l=1}^{N_i} \frac{10^{(1.5M_l + 11.8)}}{A} \qquad 3.9$$

Making $\bar{E}_T = \Im_1$ yields model 1.

3.1.2 Model 2

Equation 3.9 can be re-written as:

$$\bar{E}_T = \frac{1}{T} \sum_{l=1}^{N_i} \frac{10^{(1.5M_l + 11.8)}}{A} \qquad 3.10$$

where $M = M_w$

The G-R relation , $Log_{10}N = a - bM$ could be written as

$$N = 10^{(a-bM)} \qquad 3.11$$

This yields

$$10^{M} = 10^{(a/b)} N^{-(1/b)} \qquad 3.12$$

Substituting equation (3.12) into equation (3.10) and making $\bar{E}_T = \Im_2$ yields

$$\Im_2 = \frac{1}{TA} \sum_{i=1}^{n} \frac{10^{1.5(a_i/b_i)}}{N_i^{1/b_i}} \times 10^{11.8} \qquad 3.13$$

where

a_i , b_i , are the constants for the sub-period s_i and N_i is the number of events for the sub-period s_i. This is the second model.

3.2 Description of Data Used For The Models

The data for this work were obtained from the earthquake catalogue of the Advanced National Seismic System (ANSS), a website of Northern California Earthquake Data Centre, USA. The selected data consisted of natural earthquakes with $M \geq 1.0$ for the study areas from January 1, 1956 – January 1, 2006. The data for each earthquake consist of the following :

1. Date of occurrence
2. Time of occurrence
3. The Latitude of the epicentre.
4. The Longitude of the epicentre.
5. The depth
6. The magnitude
7. Magnitude type

3.3 Description of the Study Area

The region of study covers ten different regions in the World's seismic zones, namely Mediterranean (R1), Southern Africa (R2), West Europe (R3), West Pacific (R4), South Australia (R5), Southwest Pacific (R6), West of South America (R7), West of North America (R8), Arctic (R9) and Japan (R10). The longitudinal and latitudinal boundaries of the study area are shown in table 3.1. The locations of the regions on the global seismicity map is shown in figure 3.1

Table 3.1 Description of the Study Area

Region	Minimum Latitude	Maximum Latitude	Minimum Longitude	Maximum Longitude
R1	20	47.5	-17.5	45.5
R2	-35	-5	5	55
R3	55	70	0	49
R4	-20	5	99	150
R5	-45	-20	110	160
R6	-45	-20	160	200
R7	-45	5	-90	-60
R8	20	50	-140	-10
R9	50	68	-160	-130
R10	30	55	130	170

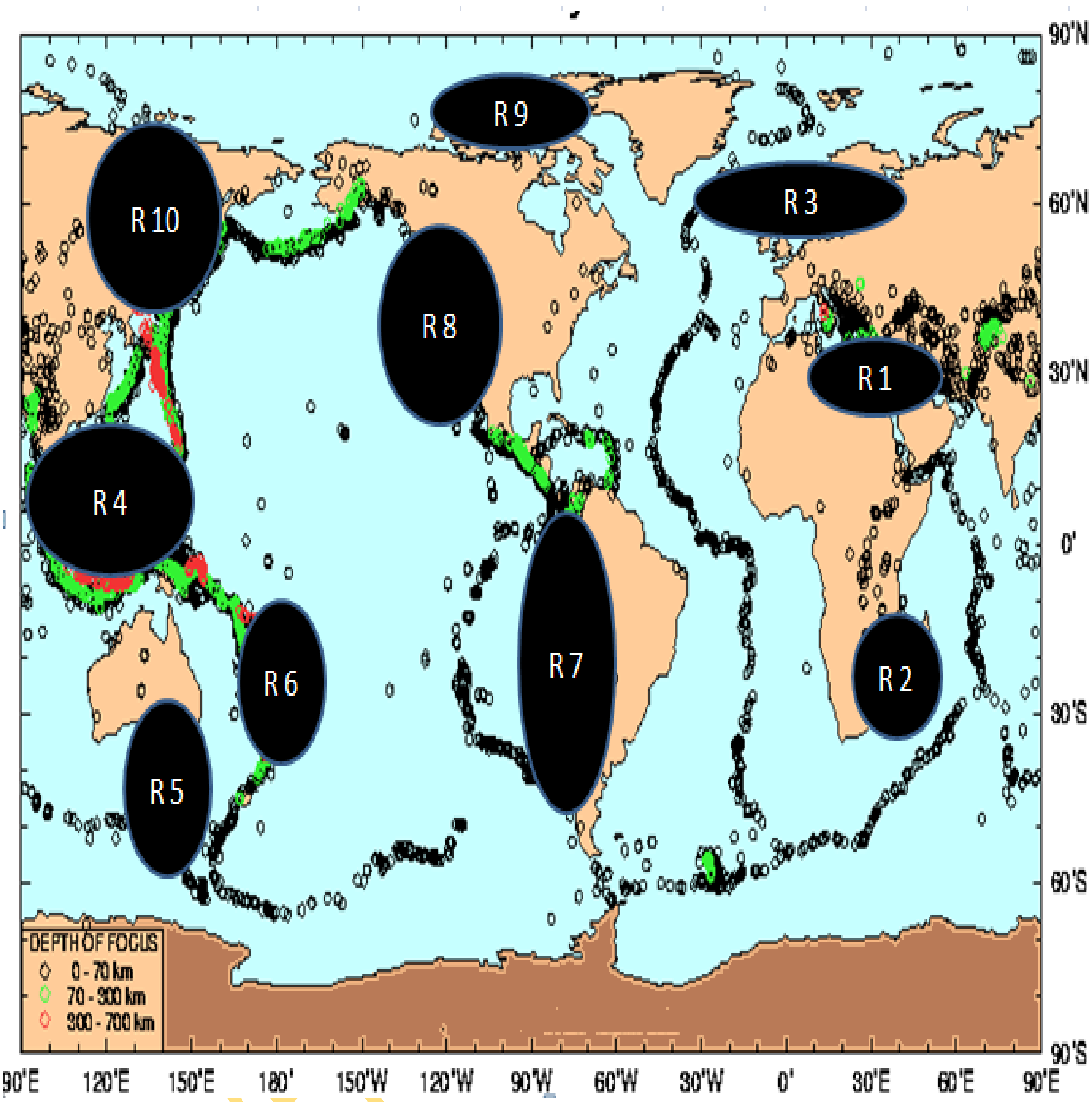

Fig.3.1: Adjusted Global Seismicity Map with the Regions of Study Inscribed

3.4 Data Treatment

In the catalogue, the earthquakes were recorded in different magnitude types. All these were converted to the moment magnitude (M_w) using the following empirical relations.

$0.80\ M_L - 0.60\ M_s = 1.04$ or $M_s = 1.33\ M_L - 1.73$ 3.14

(Ambraseys and Boomer 1990)

$M_b = M_s + 1.33,\ M_s < 2.86$ 3.15

$M_b = 0.67\ M_s + 2.28,\ 2.86 < M_s < 4.90$ 3.16

$M_b = 0.33\ M_s + 3.91,\ 4.90 < M_s < 6.27$ 3.17

$M_b = 6.00,\ 6.27 > M_s$ 3.18

$\text{Log } M_o = M_s + 18.89,\ M_s < 6.76$ 3.19

$\text{Log } M_o = 1.5\ M_s + 15.51,\ 6.76 < M_s < 8.12$ 3.20

$\text{Log } M_o = 3\ M_o + 3.33,\ 8.12 < M_s < 8.22$ 3.21

$\text{Log } M_o = 8.22,\ \log M_o > 28$ 3.22

(Geller, 1976)

$\text{Log } M_o = 1.5\ M_w + 16.1$ (Kanamori, 1977) 3.23

$M_e = 0.3 + M_s$ 3.24

(USGS)

3.5 Application of The Models To Seismic Activities of The Regions of Study

The two models were applied one by one to each of the ten regions of study described in section (3.4). Fifty period data (1956 – 2006) were taken for each region, therefore the total period, T = 50 years. The whole period was divided into five sub periods of ten years each (1956-1965, 1966-1975, 1976-1985, 1986-1995 and 1996-2005). Geographical area of each region was calculated using the standard formula (see Table 4.1 for results):

$$A = (\pi/180)R^2 \{\sin(lat1)-\sin(lat2)\} \{lon1-lon2\} \qquad 3.25$$

where lat1, lat2 are latitudinal boundaries of the region; lon1, lon2 are longitudinal boundaries of the region., R= radius of the Earth.

3.5.1 The application of Model 1

The application of model 1 for each region then took the form

$$\Im_1 = \frac{1}{50}\sum_{i=1}^{k}\frac{10^{(1.5m_i+11.8)}}{A} \qquad 3.26$$

Where m_i is the moment magnitude of each of the earthquake

3.5.2 The application of Model 2

Using the data for each of the sub periods the constants a and b were estimated from the Gutenberg-Richter magnitude- frequency relation by means of linear curve fitting. This yielded for each for each region a_i, b_i; i = 1, 2….., 5. Thus, model 2 took the following form:

$$\Im_2 = \frac{1}{50A}\sum_{j=1}^{5}\frac{10^{1.5a_j/b_j}}{N_j^{1/b_j}} \times 10^{11.8} \qquad 3.27$$

The arithmetic means of the Gutenberg-Richter constants were also calculated for the whole fifty year period. This would serve as the Gutenberg-Richter rating which would be compared with those of the two models.

3.6 Temporal Variation of the Energy density per unit time

From the values of the energy/Average Area/time obtained for each sub period, Graphs showing the temporal variation of this parameter for each of the regions were plotted in order to obtain information about the seismic activity rates for the regions. See Fig 4.1 (i-x).

CHAPTER FOUR

RESULTS AND DISCUSSION

4.1 Results

The results of the computations described in section 3.5, 3.5.1, 3.5.2 and 3.6 are presented in this chapter. This consists of calculation of the geographical area of each of the ten regions, applications of model 1 and 2 to each of ten regions of study in order to obtain the radiated energy per area per time. This is followed by the rating of seismic activities of the regions by the two models, which was the major objective of this work.

Table 4.1 presents the estimated geographical area of the ten regions of study using equation 3.25.

The values of the radiated energy per area per time obtained for regions 1 to 10 using model 1 are shown in tables 4.2 (i – x).

Table 4.3 shows the rating of seismic activities of the ten regions by model 1.

The values of the radiated energy per area per time for regions 1 to 10 using model 2 are shown in table 4.4 (i – x).

Table 4.5 shows the rating of seismic activities of the ten regions using model 2.

The values of Gutenberg–Richter's constants a and b for 5 years sub-periods for each of region 1 – 10 are shown in table 4.6 (i – x) .

Table 4.7 presents the rating of the seismic activities of the ten regions by the Gutenberg–Richter's method using the average values of constant a of each region.

Figures 4.1 (i-x) show the temporal variation of radiated energy per area for each of the ten regions for the fifty year period considered.

The discussion of these results is presented in section 4.2.

Table 4.1: Estimated Geographical Average Area coverage of the Regions Using Equation 3.25.

REGION	AVERAGE AREA COVERED (Km^2)
R1	774,912.10
R2	3,768,768.47
R3	3,207,703.96
R4	1,665,122.72
R5	2,202,775.31
R6	1,762,220.25
R7	2,301,149.14
R8	8,345,886.78
R9	4,513,027.49
R10	332,993.25

Table 4.2(i): Showing The Seismic Energy/Average Area/Time for Region 1 Using Model 1

Average Area ($10^5\,km^2$)	**Period**	**Total Number Of Events**	**Energy/Average Area/Time** $10^{13}\,J/km^2/year$ $\Im$
7.7	1956 - 1965	21345	0.00901608068
7.7	1966 - 1975	25672	0.00971711503
7.7	1976 - 1985	28412	0.01550064843
7.7	1986 - 1995	36082	0.01640939666
7.7	1996 - 2005	39715	0.01809058089
Average Value			0.01374676434

Table 4.2(ii): Showing The Seismic Energy/Average Area/Time for Region 2 Using Model 1

Average Area ($10^5 km^2$)	**Period**	**Total Number Of Events**	**Energy/Average Area/Time** $10^{13} J/km^2/year$ $\Im$
37.6	1956 - 1965	18908	0.00074206734
37.6	1966 - 1975	20980	0.00079812279
37.6	1976 - 1985	21123	0.00089688715
37.6	1986 - 1995	22768	0.00090089111
37.6	1996 - 2005	26758	0.00090222576
Average Value			0.00084803883

Table 4.2(iii): Showing The Seismic Energy/Average Area/Time for Region 3 Using Model 1

Average Area $(10^5\,km^2)$	**Period**	**Total Number Of Events**	**Energy/Average Area/Time** $10^{13}\,J/km^2/year$ $\Im$
32.0	1956 - 1965	9243	0.00228785764
32.0	1966 - 1975	9578	0.00341688951
32.0	1976 - 1985	9789	0.00429502541
32.0	1986 - 1995	10008	0.00479054495
32.0	1996 - 2005	11113	0.00506809862
Average Value			0.00397168322

Table 4.2(iv): Showing The Seismic Energy/Average Area/Time for Region 4 Using Model 1

Average Area $(10^5\,km^2)$	**Period**	**Total Number Of Events**	**Energy/Average Area/Time** $10^{13}\,J/km^2/year$ $\mathfrak{I}$
16.6	1956 - 1965	11145	0.00673638035
16.6	1966 - 1975	18799	0.00743116398
16.6	1976 - 1985	19996	0.00803532365
16.6	1986 - 1995	23456	0.00869989929
16.6	1996 - 2005	26234	0.00975717872
Average Value			0.00813198920

Table 4.2(v): Showing The Seismic Energy/Average Area/Time for Region 5 Using Model 1

Average Area $(10^5\,km^2)$	**Period**	**Total Number Of Events**	**Energy/Average Area/Time** $10^{13} J/km^2/year$ $\Im$
22.0	1956 - 1965	12453	0.00510358452
22.0	1966 - 1975	18999	0.00520862474
22.0	1976 - 1985	22671	0.00735509877
22.0	1986 - 1995	25989	0.00741218584
22.0	1996 - 2005	28999	0.00744872157
Average Value			0.00650564309

Table 4.2(vi): Showing The Seismic Energy/Average Area/Time for Region 6 Using Model 1

Average Area $(10^5\,km^2)$	**Period**	**Total Number Of Events**	**Energy/Average Area/Time** $10^{13}\,J/km^2/year$ $\Im$
17.6	1956 - 1965	14109	0.00364215540
17.6	1966 - 1975	16563	0.00629955875
17.6	1976 - 1985	19652	0.00669631392
17.6	1986 - 1995	28769	0.00959062863
17.6	1996 - 2005	29876	0.00963058958
Average Value			0.00717184926

Table 4.2(vii): Showing The Seismic Energy/Average Area/Time for Region 7 Using Model 1

Average Area ($10^5\,km^2$)	**Period**	**Total Number Of Events**	**Energy/Average Area/Time** $10^{13}\,J/km^2/year$ $\mathfrak{I}$
23.0	1956 - 1965	12075	0.00357607416
23.0	1966 - 1975	13720	0.00497721325
23.0	1976 - 1985	17111	0.00558706942
23.0	1986 - 1995	19331	0.00611823447
23.0	1996 - 2005	22001	0.00641114030
Average Value			0.00533394632

Table 4.2(viii): Showing The Seismic Energy/Average Area/Time for Region 8 Using Model 1

Average Area $(10^5 km^2)$	**Period**	**Total Number Of Events**	**Energy/Average Area/Time** $10^{13} J/km^2/year$ $\Im$
83.4	1956 - 1965	15463	0.00147358218
83.4	1966 - 1975	18076	0.00181530859
83.4	1976 - 1985	20412	0.00194307932
83.4	1986 - 1995	22167	0.00260423255
83.4	1996 - 2005	23242	0.00300803625
Average Value			0.00216884778

Table 4.2(ix): Showing The Seismic Energy/Average Area/Time for Region 9 Using Model 1

Average Area ($10^5\,km^2$)	**Period**	**Total Number Of Events**	**Energy/Average Area/Time** $10^{13}\,J/km^2/year$ $\Im$
45.1	1956 - 1965	18763	0.00132520132
45.1	1966 - 1975	22456	0.00144557285
45.1	1976 - 1985	25670	0.00270835931
45.1	1986 - 1995	27659	0.00275182680
45.1	1996 - 2005	28945	0.00298922620
Average Value			0.00224403730

Table 4.2(x): Showing The Seismic Energy/Average Area/Time for Region 10 Using Model 1

Average Area $(10^5\,km^2)$	**Period**	**Total Number Of Events**	**Energy/Average Area/Time** $10^{13}\,J/km^2/year$ $\Im$
3.3	1956 - 1965	11895	0.02101162722
3.3	1966 - 1975	12754	0.03563366543
3.3	1976 - 1985	19867	0.03783905549
3.3	1986 - 1995	20986	0.04424374991
3.3	1996 - 2005	21456	0.04924364107
Average Value			0.03759434782

Table 4.3: Showing Seismic Activity Rating of the Regions in descending order using Model 1

SEISMICITY RATING	ENERGY/AVERAGE AREA/TIME $10^{13} J/km^2/year$ $\Im$	REGION
10	0.0375	R10
9	0.0137	R1
8	0.0081	R4
7	0.0071	R6
6	0.0065	R5
5	0.0053	R7
4	0.0039	R3
3	0.0022	R9
2	0.0021	R8
1	0.0008	R2

Table 4.4(i): Showing the Seismic energy/Average area/Time for region 1 using Model 2

Average Area ($10^5\,km^2$)	Period	Total Number Of Events	A	B	Energy/Average Area $10^{13} J/km^2$	Energy/Average Area/Time $10^{13} J/km^2/year$ $\Im$
7.7	1956 – 1965	21345	5.21	0.85	0.430208083	0.043020808
7.7	1966 – 1975	25672	5.57	0.89	0.46127302	0.046127302
7.7	1976 – 1985	28412	6.51	1.05	0.718527543	0.071852754
7.7	1986 – 1995	36082	6.99	1.12	0.759000322	0.075900032
7.7	1996 – 2005	39715	6.72	1.04	0.775999697	0.07759997
Average Value			6.20	0.99	0.629001733	0.062900173

Table 4.4(ii): Showing the Seismic energy/Average area/Time for region 2 using Model 2

Average Area ($10^5 km^2$)	**Period**	**Total Number Of Events**	**A**	**B**	**Energy/Average Area $10^{13} J/km^2$**	**Energy/Average Area/Time $10^{13} J/km^2/year$ $\Im$**
37.6	1956 - 1965	18908	4.65	0.62	0.188873148	0.018887315
37.6	1966 - 1975	20980	4.9	0.63	0.200938733	0.020093873
37.6	1976 - 1985	21123	5.23	0.69	0.208543359	0.020854336
37.6	1986 - 1995	22768	5.16	0.62	0.216429852	0.021642985
37.6	1996 - 2005	26758	5.38	0.65	0.220214908	0.022021491
Average Value			5.06	0.64	0.207	0.0207

Table 4.4(iii): Showing The Seismic Energy/Average Area/Time for Region 3 using Model 2

Average Area ($10^5\ km^2$)	**Period**	**Total Number Of Events**	**A**	**B**	**Energy/Average Area** $10^{13}J/km^2$	**Energy/Average Area/Time** $10^{13}J/km^2/year$ $\Im$
32.0	1956 – 1965	9243	2.85	0.37	0.179756988	0.017975699
32.0	1966 – 1975	9578	3.07	0.35	0.274247768	0.027424777
32.0	1976 – 1985	9789	3.44	0.4	0.327251025	0.032725102
32.0	1986 – 1995	10008	3.5	0.36	0.375147574	0.037514757
32.0	1996 – 2005	11113	3.98	0.43	0.418596645	0.041859664
Average Value			3.37	0.38	0.315	0.0315

Table 4.4(iv): Showing The Seismic Energy/Average Area/Time for Region 4 using Model 2

Average Area ($10^5\,km^2$)	**Period**	**Total Number Of Events**	**A**	**B**	**Energy/Average Area** $10^{13}J/km^2$	**Energy/Average Area/Time** $10^{13}J/km^2/year$ $\Im$
16.6	1956 - 1965	11145	3.8	0.62	0.5311	0.0531
16.6	1966 - 1975	18799	3.96	0.61	0.5893	0.0589
16.6	1976 - 1985	19996	4.36	0.66	0.5934	0.0593
16.6	1986 - 1995	23456	4.55	0.67	0.6396	0.064
16.6	1996 - 2005	26234	5.54	0.82	0.7516	0.0752
Average Value			4.44	0.68	0.621	0.0621

Table 4.4(v): Showing The Seismic Energy/Average Area/Time for Region 5 using Model 2

Average Area ($10^5\,km^2$)	Period	Total Number Of Events	A	B	Energy/Average Area $10^{13}J/km^2$	Energy/Average Area/Time $10^{13}J/km^2/year$ $\mathfrak{I}$
22.0	1956 - 1965	12453	3.73	0.46	0.392	0.0392
22.0	1966 - 1975	18999	4.75	0.64	0.4691	0.0469
22.0	1976 – 1985	22671	4.75	0.63	0.5363	0.0536
22.0	1986 - 1995	25989	4.74	0.62	0.5778	0.0578
22.0	1996 - 2005	28999	4.82	0.63	0.6047	0.0605
Average Value			4.56	0.60	0.516	0.0516

Table 4.4(vi): Showing The Seismic Energy/Average Area/Time for Region 6 using Model 2

Average Area ($10^5\, km^2$)	Period	Total Number Of Events	A	B	Energy/Average Area $10^{13} J/km^2$	Energy/Average Area/Time $10^{13} J/km^2/year$ $\Im$
17.6	1956 - 1965	14109	4.1	0.91	0.3489	0.0349
17.6	1966 - 1975	16563	4.31	0.93	0.4096	0.041
17.6	1976 - 1985	19652	4.51	0.92	0.486	0.0486
17.6	1986 - 1995	28769	4.72	0.92	0.7115	0.0712
17.6	1996 - 2005	29876	4.91	0.96	0.7389	0.0739
Average Value			4.51	0.93	0.539	0.0539

Table 4.4(vii): Showing The Seismic Energy/Average Area/Time for Region 7 using Model 2

Average Area ($10^5\,km^2$)	**Period**	**Total Number Of Events**	**A**	**B**	**Energy/Average Area** $10^{13}J/km^2$	**Energy/Average Area/Time** $10^{13}J/km^2/year$ $\Im$
23.0	1956 - 1965	12075	1.93	0.33	0.3229	0.0323
23.0	1966 - 1975	13720	3.1	0.51	0.3775	0.0377
23.0	1976 - 1985	17111	3.98	0.65	0.4263	0.0426
23.0	1986 - 1995	19331	4.09	0.67	0.4629	0.0463
23.0	1996 - 2005	22001	4.52	0.76	0.4854	0.0485
Average Value			3.52	0.58	0.415	0.0415

Table 4.4(viii): Showing The Seismic Energy/Average Area/Time for Region 8 using Model 2

Average Area ($10^5 km^2$)	**Period**	**Total Number Of Events**	**A**	**B**	**Energy/Average Area** $10^{13} J/km^2$	**Energy/Average Area/Time** $10^{13} J/km^2/year$ $\Im$
83.4	1956 - 1965	15463	3.58	0.52	0.2145	0.0215
83.4	1966 - 1975	18076	3.91	0.53	0.258	0.0258
83.4	1976 - 1985	20412	4	0.53	0.2856	0.0286
83.4	1986 - 1995	22167	4.11	0.54	0.3627	0.0363
83.4	1996 - 2005	23242	4.13	0.53	0.3992	0.0399
Average Value			3.95	0.53	0.304	0.0304

Table 4.4(ix): Showing The Seismic Energy/Average Area/Time for Region 9 using Model 2

Average Area ($10^5\ km^2$)	**Period**	**Total Number Of Events**	**A**	**B**	**Energy/Average Area** $10^{13} J/km^2$	**Energy/Average Area/Time** $10^{13} J/km^2/year$ $\Im$
45.1	1956 - 1965	18763	5.21	0.85	0.2086	0.0209
45.1	1966 - 1975	22456	5.57	0.89	0.2237	0.0224
45.1	1976 - 1985	25670	6.51	1.05	0.3484	0.0348
45.1	1986 - 1995	27659	6.99	1.12	0.368	0.0368
45.1	1996 - 2005	28945	6.72	1.04	0.3763	0.0376
Average Value			6.20	0.99	0.305	0.0305

Table 4.4(x): Showing The Seismic Energy/Average Area/Time for Region 1 using Model 2

Average Area ($10^5\,km^2$)	Period	Total Number Of Events	A	B	Energy/Average Area $10^{13}J/km^2$	Energy/Average Area/Time $10^{13}J/km^2/year$ $\Im$
3.3	1956 – 1965	11895	3.46	0.55	0.4676	0.0468
3.3	1966 – 1975	12754	3.48	0.55	0.7887	0.0789
3.3	1976 - 1985	19867	3.56	0.56	0.8389	0.0839
3.3	1986 - 1995	20986	4.07	0.66	0.9841	0.0984
3.3	1996 - 2005	21456	4.05	0.65	1.1007	0.1101
Average Value			3.72	0.59	0.836	0.0836

Table 4.5: Showing Seismicity Activity Rating of The Regions in descending order using Model 2.

SEISMICITY RATING	**ENERGY/AVERAGE AREA/TIME** $10^{13} J/km^2/year$ $\Im$	**REGION**
10	0.0836	R10 (highest)
9	0.0629	R1
8	0.0621	R4
7	0.0539	R6
6	0.0516	R5
5	0.0415	R7
4	0.0315	R3
3	0.0305	R9
2	0.0304	R8
1	0.0207	R2 (least)

Table 4.6 (i): Estimated G-R Constants for Region 1.

Time Interval	a	b
1956 – 1966	5.21	0.85
1967 – 1976	5.57	0.89
1977 – 1986	6.51	1.05
1987 – 1996	6.99	1.12
1997 – 2006	6.72	1.04
Average Value	**6.20**	**0.99**

Table 4.6 (ii): Estimated G-R Constants for Region 2

Time Interval	a	b
1956 – 1966	4.65	0.62
1967 – 1976	4.9	0.63
1977 – 1986	5.23	0.69
1987 – 1996	5.16	0.62
1997 – 2006	5.38	0.65
Average Value	**5.06**	**0.64**

Table 4.6 (iii): Estimated G-R Constants for Region 3.

Time Interval	a	b
1956 - 1966	2.85	0.37
1967 – 1976	3.07	0.35
1977 – 1986	3.44	0.4
1987 – 1996	3.5	0.36
1997 – 2006	3.98	0.43
Average Value	**3.37**	**0.38**

Table 4.6 (iv): Estimated G-R Constants for Region 4.

Time Interval	a	b
1956 – 1966	3.8	0.62
1967 – 1976	3.96	0.61
1977 – 1986	4.36	0.66
1987 – 1996	4.55	0.67
1997 – 2006	5.54	0.82
Average Value	**4.44**	**0.68**

Table 4.6 (v): Estimated G-R Constants for Region 5.

Time Interval	a	b
1956 - 1966	3.73	0.46
1967 - 1976	4.75	0.64
1977 - 1986	4.75	0.63
1987 - 1996	4.74	0.62
1997 - 2006	4.82	0.63
Average Value	**4.56**	**0.60**

Table 4.6 (vi): Estimated G-R Constants for Region 6.

Time Interval	**a**	**b**
1956 – 1966	4.1	0.91
1967 – 1976	4.31	0.93
1977 – 1986	4.51	0.92
1987 – 1996	4.72	0.92
1997 – 2006	4.91	0.96
Average Value	**4.51**	**0.93**

Table 4.6 (vii): Estimated G-R Constants for Region 7.

Time Interval	a	b
1956 – 1966	1.93	0.33
1967 - 1976	3.1	0.51
1977 - 1986	3.98	0.65
1987 - 1996	4.09	0.67
1997 - 2006	4.52	0.76
Average Value	**3.52**	**0.58**

Table 4.6 (viii): Estimated G-R Constants for Region 8.

Time Interval	a	b
1956 - 1966	3.58	0.52
1967 - 1976	3.91	0.53
1977 - 1986	4	0.53
1987 - 1996	4.11	0.54
1997 - 2006	4.13	0.53
Average Value	**3.95**	**0.53**

Table 4.6 (ix): Estimated G-R Constants for Region 9.

Time Interval	a	b
1956 - 1966	5.21	0.85
1967 - 1976	5.57	0.89
1977 - 1986	6.51	1.05
1987 - 1996	6.99	1.12
1997 - 2006	6.72	1.04
Average Value	**6.20**	**0.99**

Table 4.6 (x): Estimated G-R Constants for Region 10.

Time Interval	a	b
1956 - 1966	3.46	0.55
1967 - 1976	3.48	0.55
1977 - 1986	3.56	0.56
1987 - 1996	4.07	0.66
1997 - 2006	4.05	0.65
Average Value	**3.72**	**0.59**

Table 4.7: Seismic Activity Rating of The Regions Using Gutenberg-Richer Constant a.

SEISMIC ACTIVITY RATING	G-R CONSTANT a	REGION
10	6.20	R1(highest)
9	6.20	R9
8	5.06	R2
7	4.56	R5
6	4.51	R6
5	4.44	R4
4	3.95	R8
3	3.72	R10
2	3.52	R7
1	3.37	R3 (least)

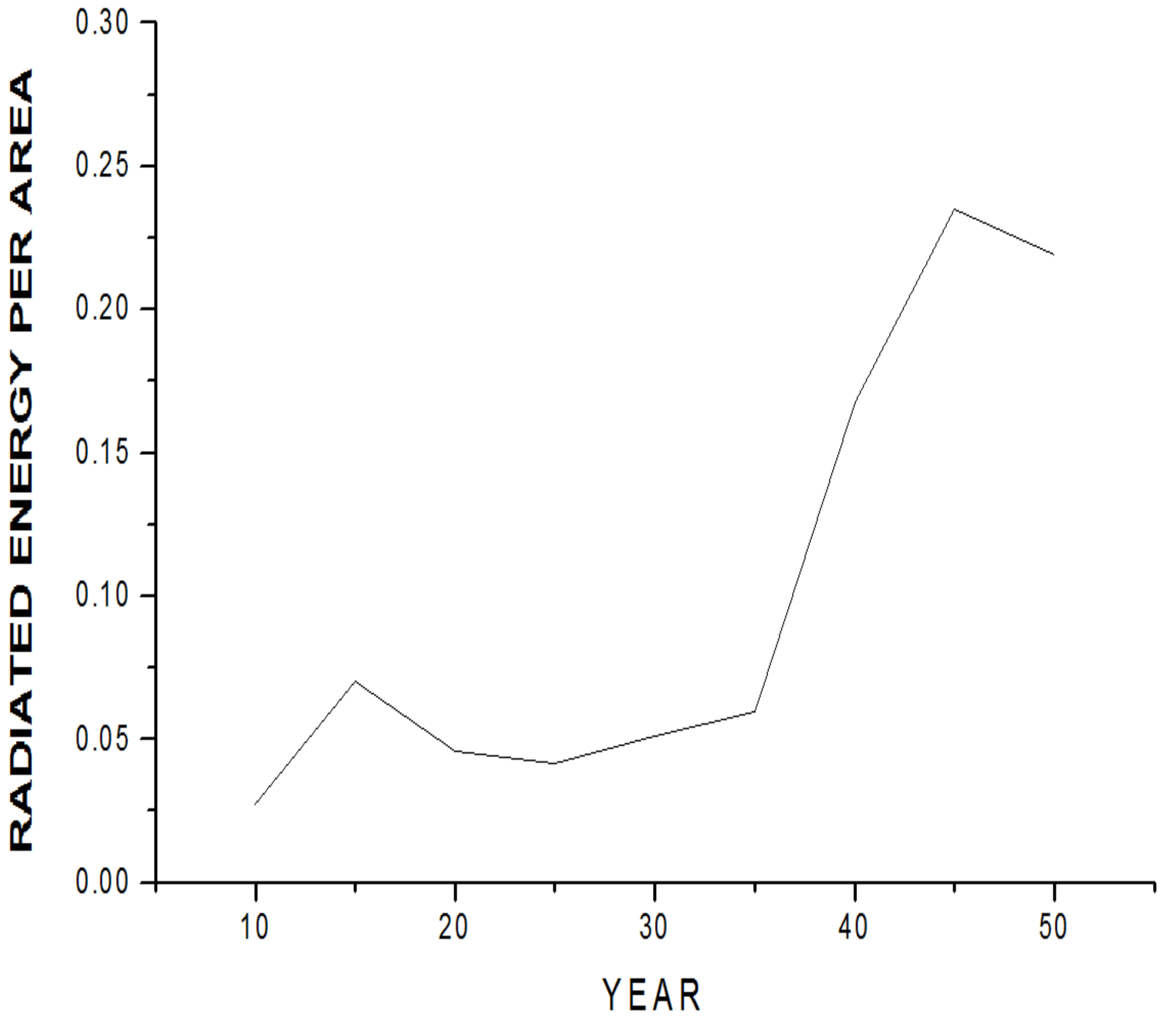

Fig. 4.1 (i): Showing Radiated Energy per Area against Time for Region 1.

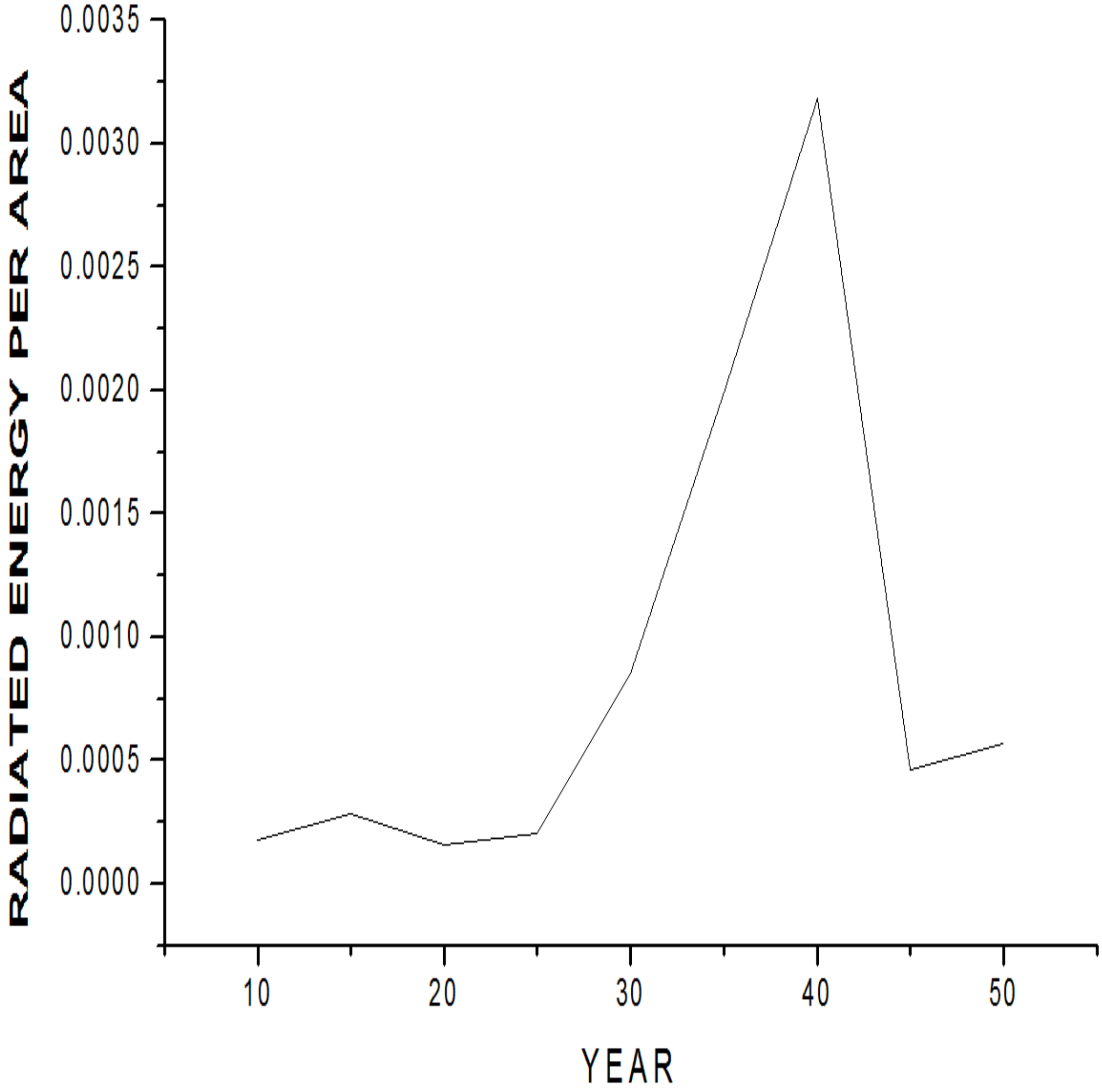

Fig. 4.1 (ii): Showing Radiated Energy per Area against Time for Region 2

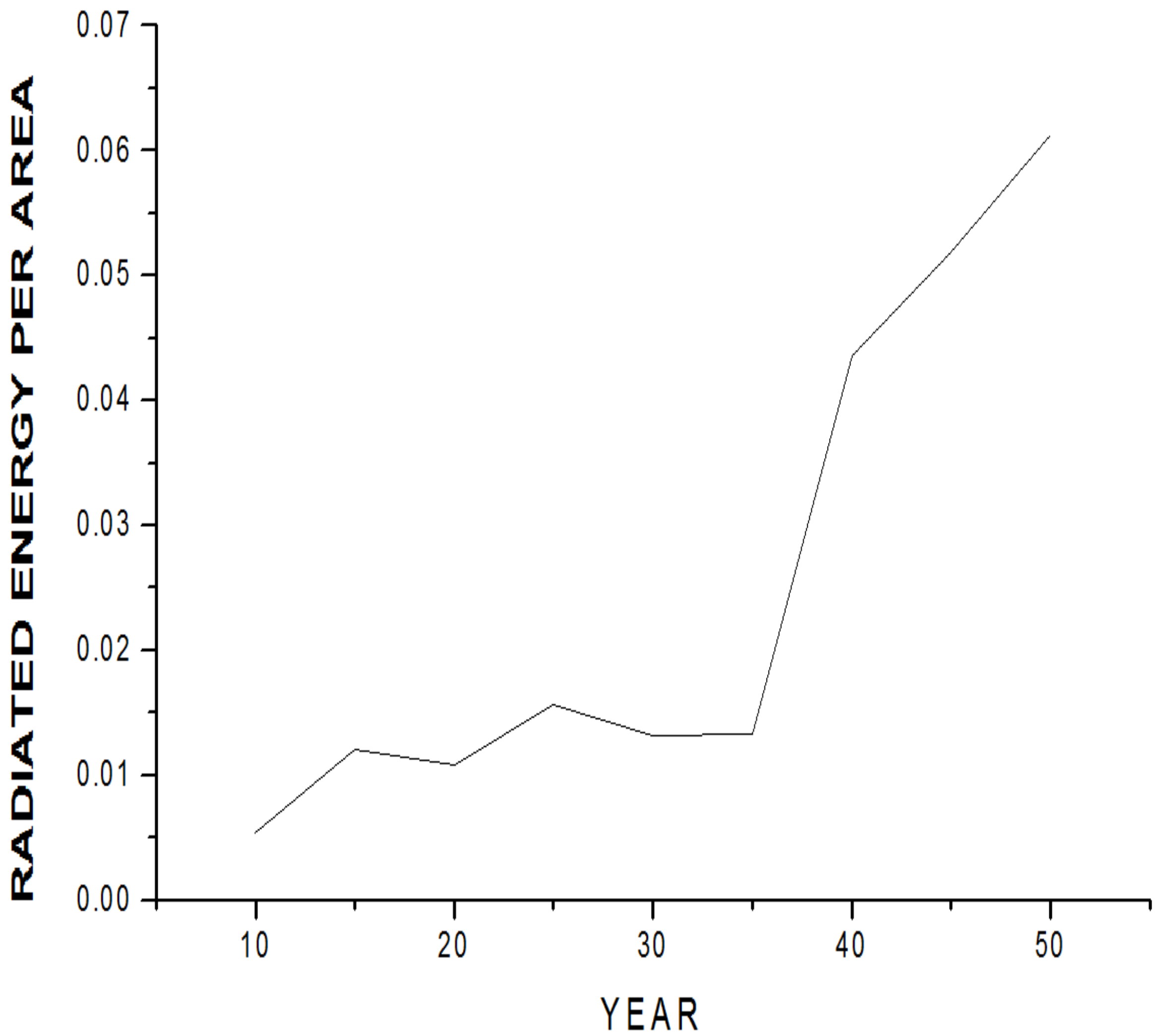

Fig. 4.1 (iii): Showing Radiated Energy per Area against Time for Region 3.

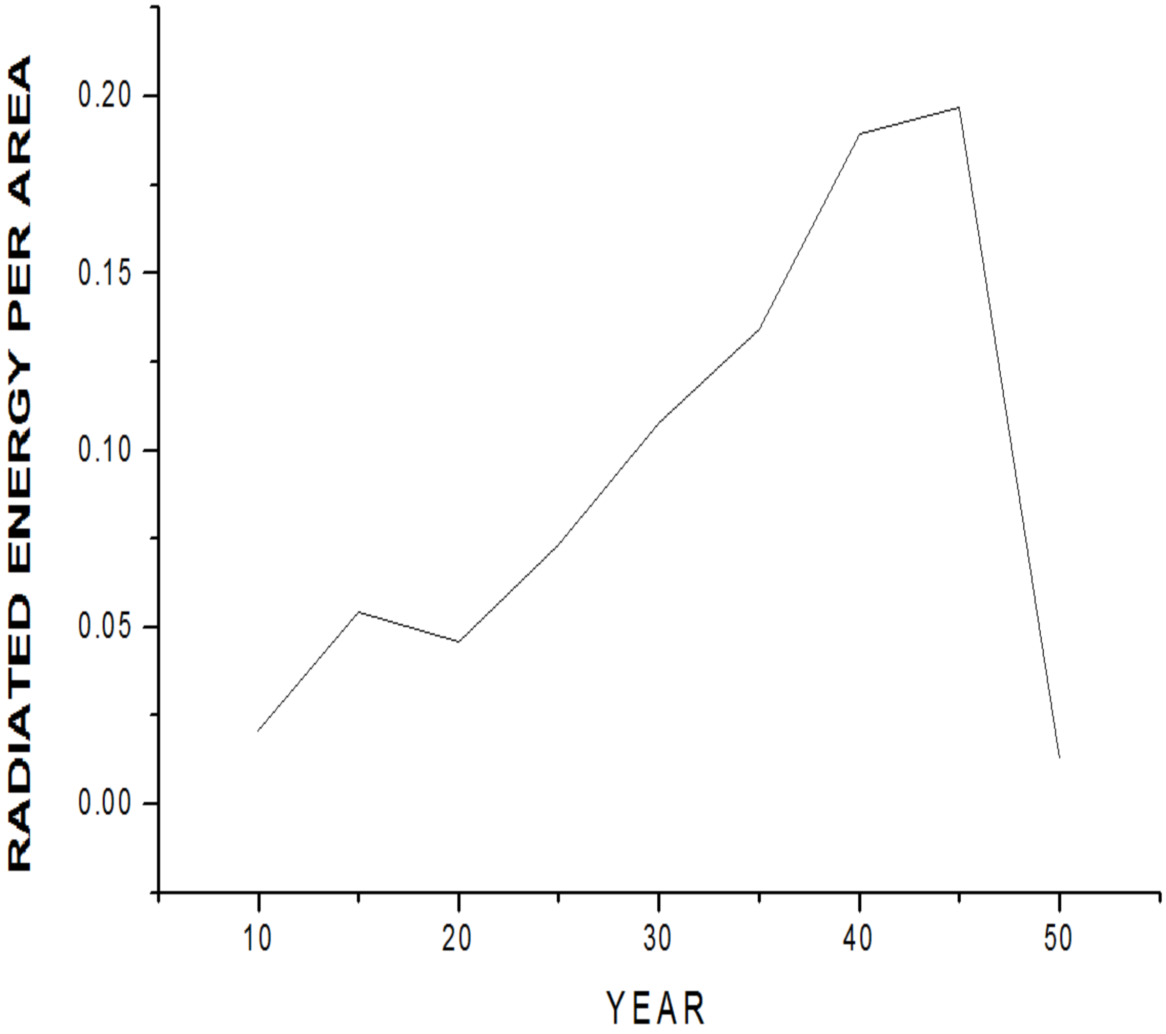

Fig. 4.1 (iv): Showing Radiated Energy per Area against Time for Region 4.

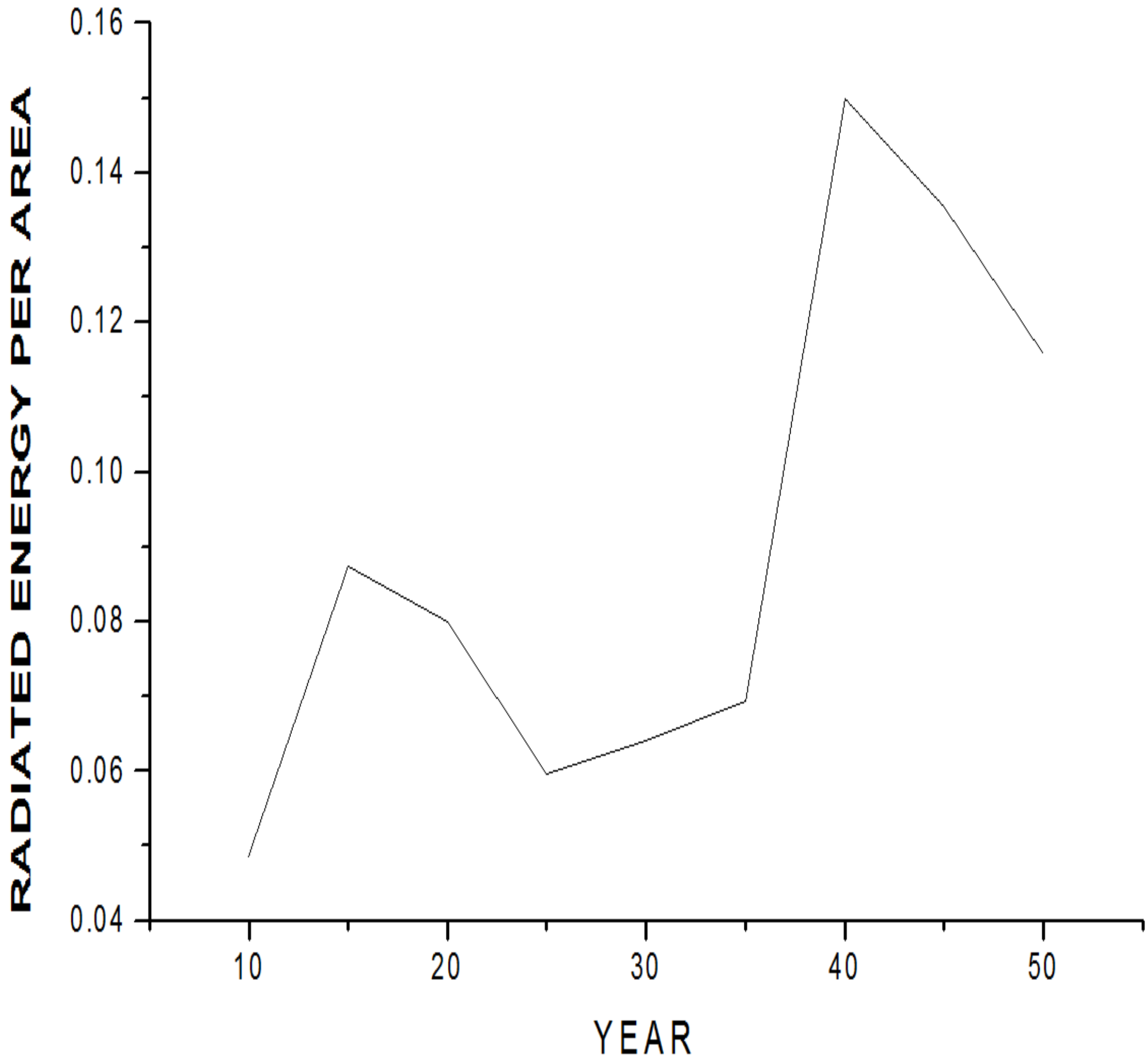

Fig. 4.1 (v): Showing Radiated Energy per Area against Time for Region 5.

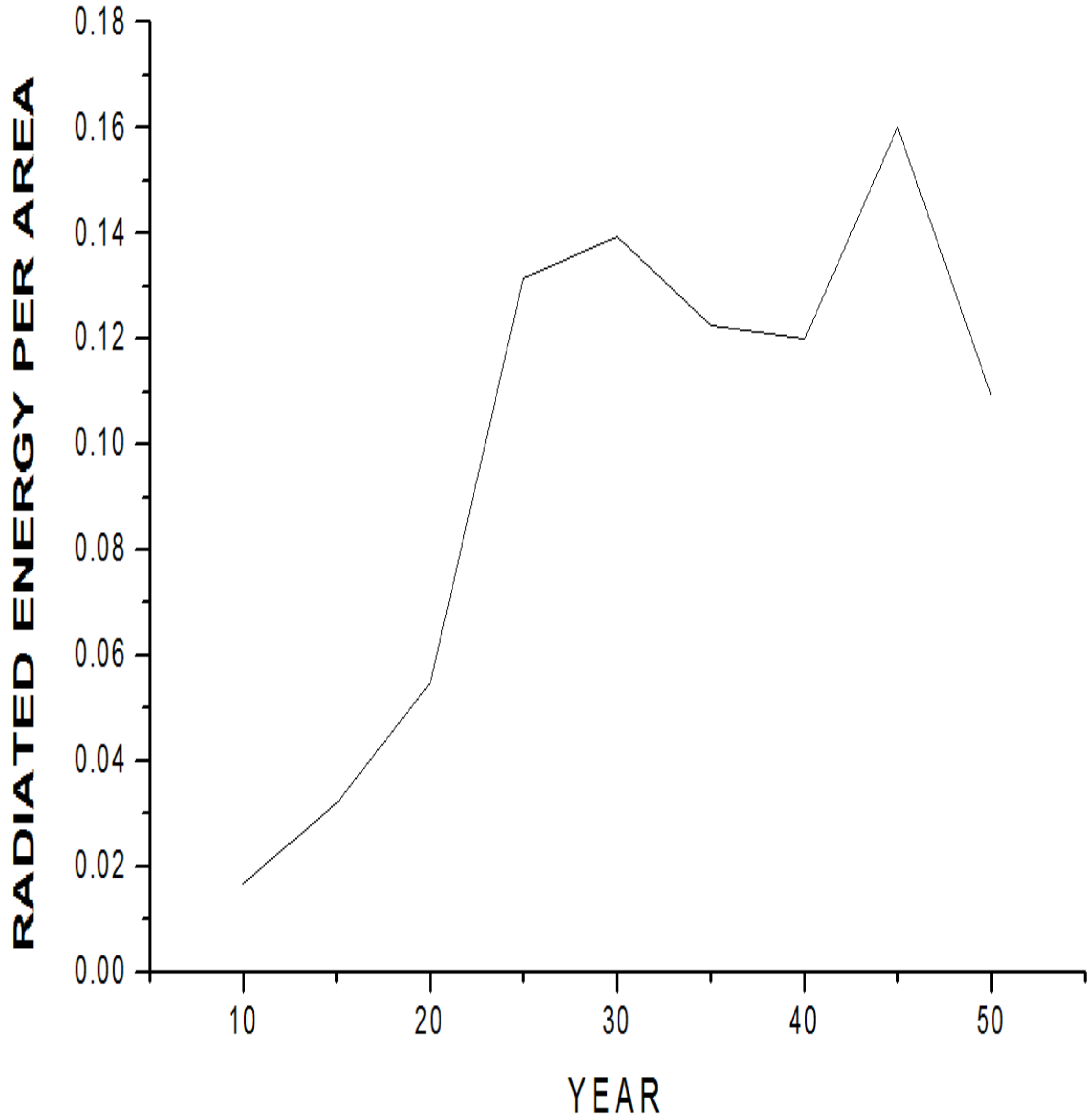

Fig. 4.1 (vi): Showing Radiated Energy per Area against Time for Region 6

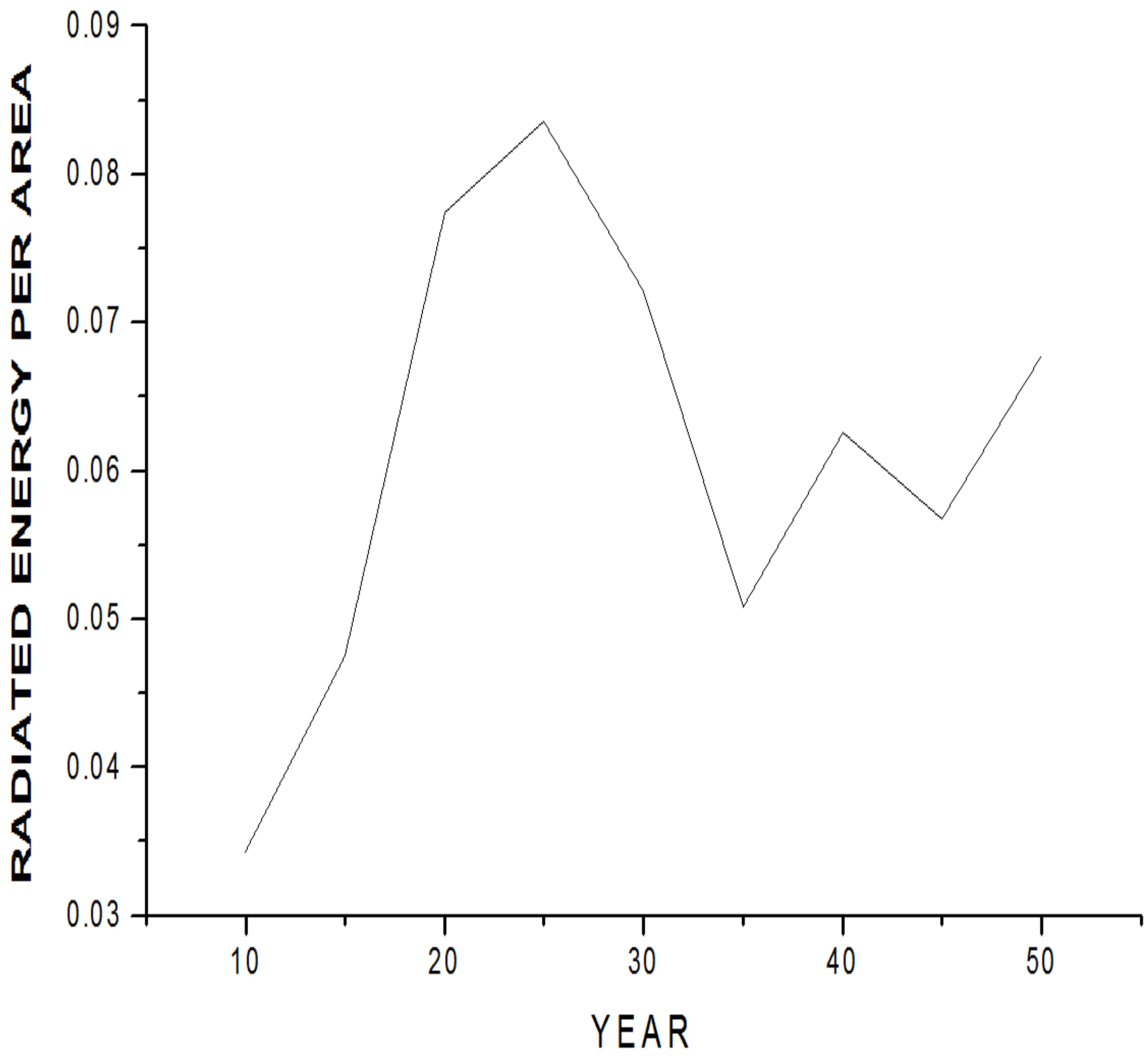

Fig. 4.1 (vii): Showing Radiated Energy per Area against Time for Region 7.

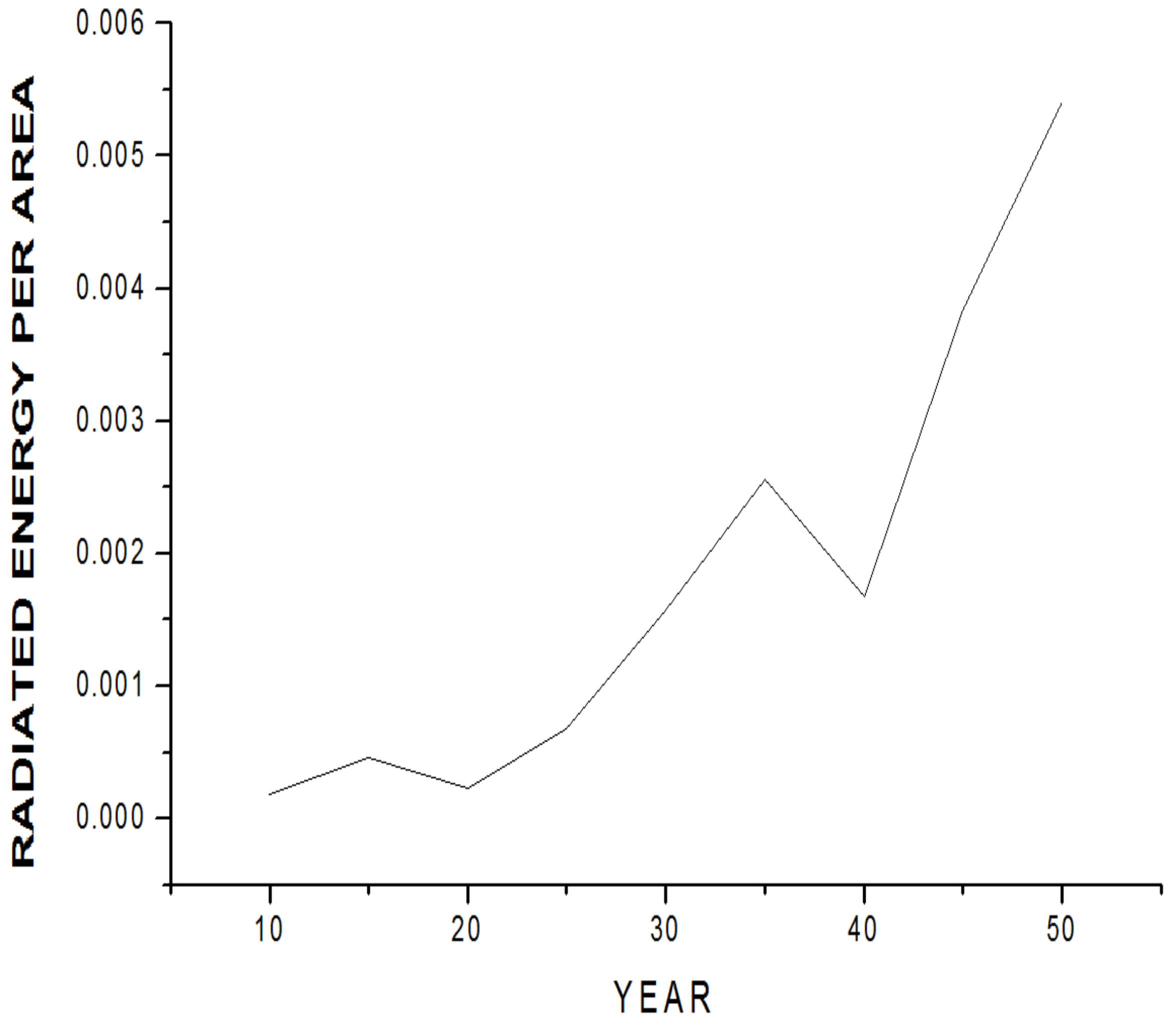

Fig. 4.1 (viii): Showing Radiated Energy per Area against Time for Region 8

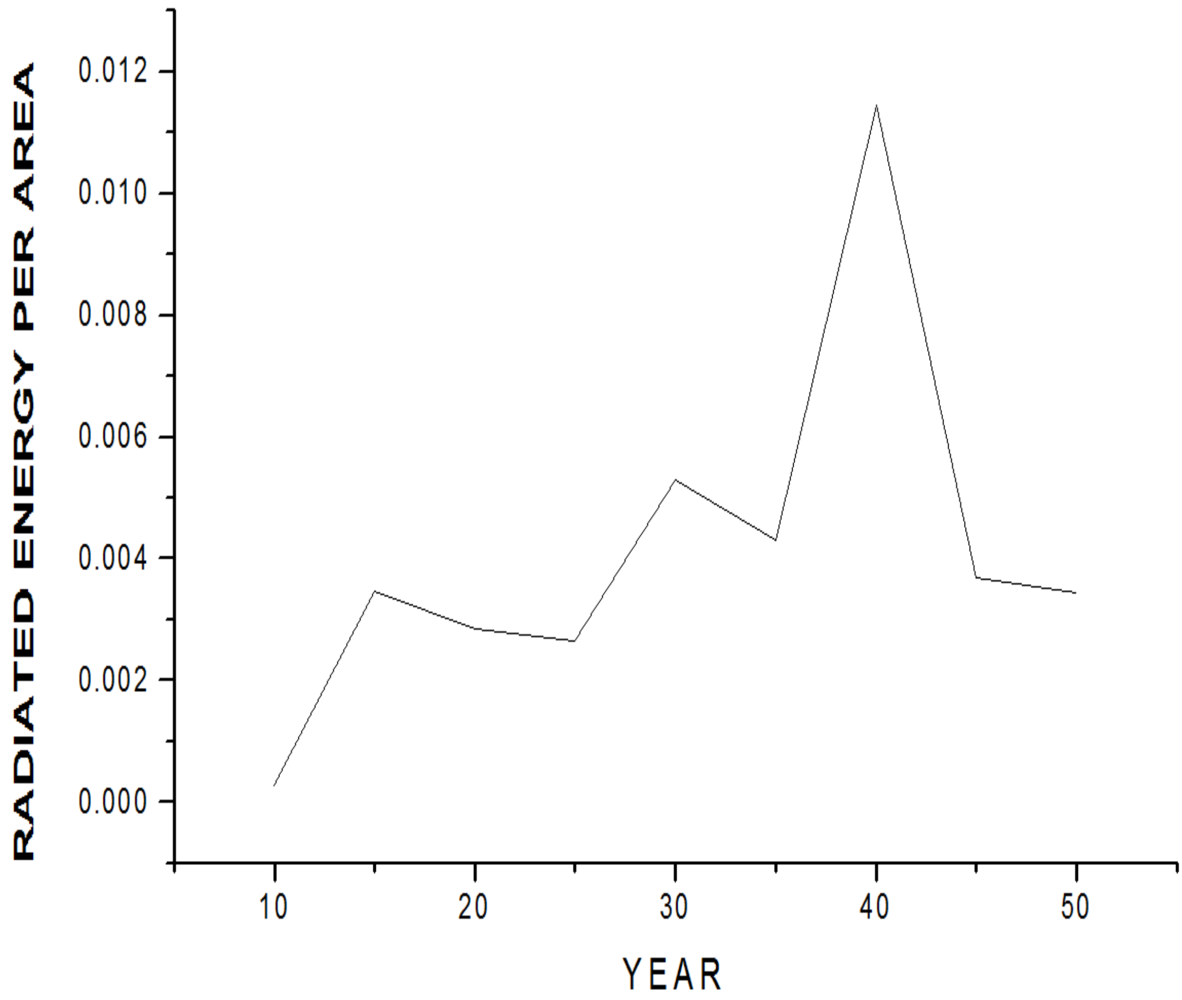

Fig. 4.1 (ix): Showing Radiated Energy per Area against Time for Region 9

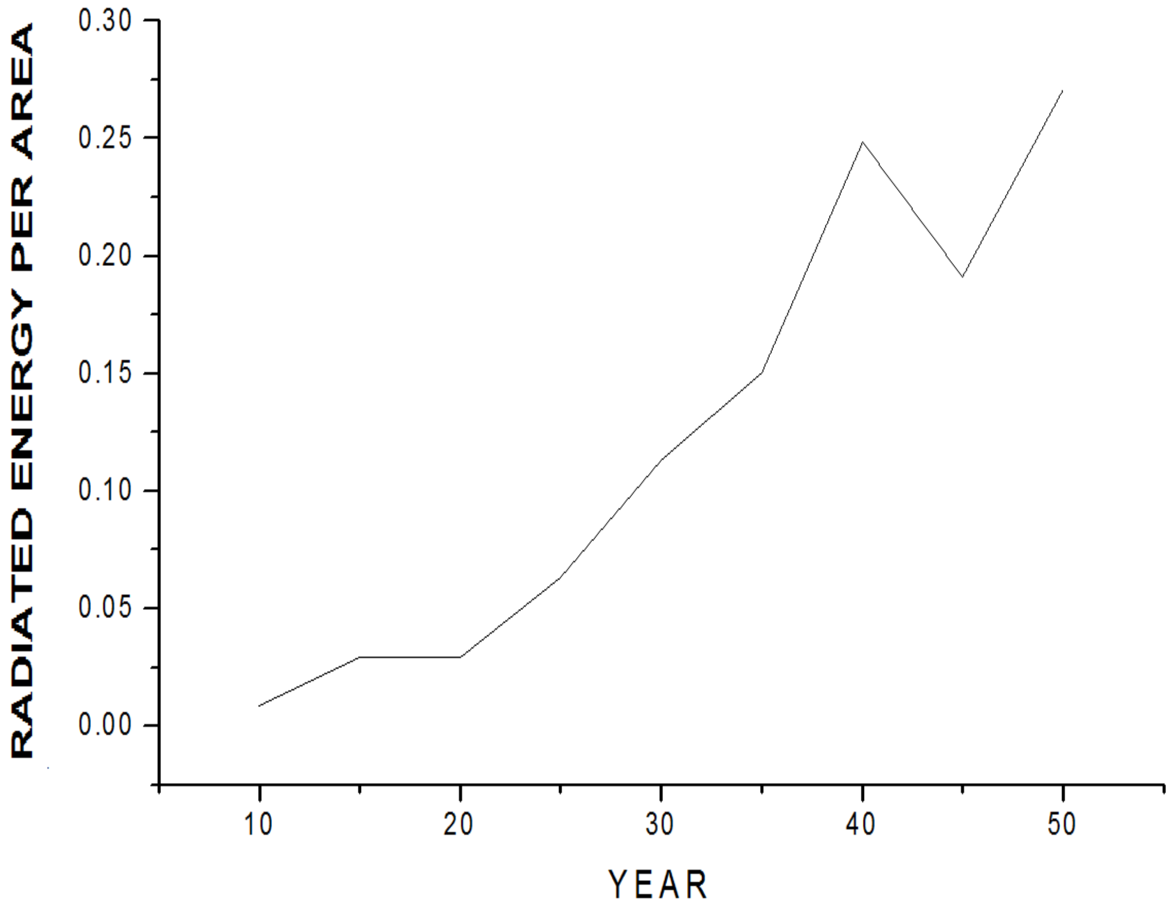

Fig. 4.1 (x): Showing Radiated Energy per Area against Time for Region 10.

4.2 DISCUSSION

Table 4.1 is very significant in the determination of the seismic activity rating of the ten regions because it takes care of one of the limitations of Gutenberg-Richter relation as a tool for the assessment of seismic activities which is non-consideration of area of the region concerned. The estimated average areas were calculated using equation 3.25 for each of the ten selected regions. The result ranked the regions in the descending order of geographical area coverage as Rg8, Rg9, Rg2, Rg3, Rg7, Rg5, Rg6, Rg4, Rg1 and Rg10.

Both model 1 and model 2 rated the seimic activities of the ten regions as Rg2 < Rg8 < Rg9 < Rg3 < Rg7 < Rg5 < Rg6 < Rg4 < Rg1 < Rg10 while Gutenberg-Richter relation rated the same ten regions of study as Rg3 < Rg7 < Rg10 < Rg8 < Rg4 < Rg6 < Rg5< Rg2 < Rg9< Rg1. The Gutenberg-Richter assessment is based on the number of total earthquakes of mixed magnitudes (which is what constant a represents) in which area coverage is not taken into consideration. Therefore Region 10 for instance is rated less than Region 2 by the Gutenberg-Richter relation.

The similarity in the rating by model 1 and model 2 is expected since both are derived from common parameter namely radiated energy of earthquakes. However, both model 1 and model 2 do not give the same values of radiated energy per area per time. This is due to the fact that the constants a and b incorporated into model 2 have been estimated by linear curve fittings in which constant a is obtained by extrapolation based on the idea that lower magnitude events are under-reported. This makes each value of radiated energy per area per time for model 2 to be greater than that of model 1.

One advantage of model 2 is that it can be used to quickly rate activities of regions where the values of Gutenberg-Richter constants a and b had been reliably determined for events over a known period of time while model 1 has the advantage of being applicable in situations where the Gutenberg-Richter constants a and b are indeterminate, for instance if the magnitude values of all events in a region are extremely close to one another.

The graphs in fig 4.1 (i-x) showed that the radiated energy per area generally increase with time in all the regions of study, in other words, seismic activity is generally on the increase in all the regions, this implies that the lithospheric layer is becoming more unstable.

Another common feature of the temporal variation radiated energy was that certain peaks are followed by falls e.g. Points (0.25,39) of fig. 4.1 (x); (0.012,38) of fig. 4.1. (ix); (0.20,45) of fig 4.1 (iv). From the earthquake catalogue, it was confirmed that this behavior is due to release of large earthquakes of magnitude 5 and above. Thus it can be deduced that the occurrence of large earthquake is usually followed by decrease in lithospheric energy flow which is evident by decrease in seismicity rate. However, radiated energy resulting from a large number of small earthquakes do not produce these observed peak and fall trends but yields pattern which vary from one region to another e.g. Points (0.01,15) of fig 4.1 (iii); (0.0005,15) of fig 4.1 (viii).

Hence, it may be deduced that there is no common pattern of radiated energy of earthquakes for different regions as different patterns should be expected as long as earthquakes magnitudes do not exceed certain optimum magnitude value of 5.

CHAPTER FIVE

SUMMARY AND CONCLUSION

In seismology, seismic activity evaluation is usually carried out using the Gutenberg-Richter's (G-R) relation. The a-value indicates the total seismicity rate of the region. This method is insufficient for rating seismic activities of two or more regions because of the following limitations:

1. G-R empirical relation does not include area of the region involved, thereby making a small but active regions to be underrated.
2. G-R empirical relation gives the rate of seismicity of a region in terms of the total number, N, of earthquakes irrespective of magnitudes. This makes regions with few but great earthquakes to be underestimated since the energy E, radiated by an earthquake of magnitude m is 10^m.

Assessment of seismic activities of regions in terms of total radiated energy of earthquakes will make comparison reliable because each earthquake magnitude will be converted to its equivalent energy.

Two models based on the estimation of total radiated energy of earthquakes per area per time were developed. This first model does not contain a and b at all, hence it takes care of all categories of magnitude spread including those for which Gutenberg-Richter's constants are indeterminate. The second model incorporates the Gutenberg-Richter's constants a and b to facilitate quick assessment of regions whose constants a and b had earlier been determined.

The two models were applied to ten regions in the world seismic zones using earthquakes data for the period 1956 to 2005. The ten regions are Mediterranean (Rg1), Southern Africa (Rg2), West Europe (Rg3), West Pacific (Rg4), South Australia (Rg5), Southwest Pacific (Rg6), West of South America (Rg7), West of North America (Rg8), Arctic (Rg9) and Japan (Rg10).

Each of the two models rated the regions of study in the same order as Rg2 < Rg8 < Rg9 < Rg3 < Rg7 < Rg5 < Rg6 < Rg4 < Rg1 < Rg10. Meanwhile the Gutenberg-Richter relation rated the regions as Rg3 < Rg7 < Rg10 < Rg8 < Rg4 < Rg6 < Rg5< Rg2 < Rg9< Rg1.

It is evident from the results that the Gutenberg-Richter constant a is insufficient for comparing seismic activities. For instance, contrary to the rating by Gutenberg-Richter method, the region of Japan (Rg10) is known to be more active than Southern Africa (Rg2). Therefore, by computing radiated energy of earthquake per area per time, it is possible to compare the seismic activities of any two or more regions of interest. This approach does more justice to seismic activity assessment since it goes beyond the count of number of earthquakes of mixed magnitudes (the Gutenberg-Richter constant a is a measure of the total number of earthquakes of different magnitudes) and it incorporates the geographical area of the region of study.

The two models developed in this work rated the regions of study in the same order, placing region 10 as the highest and region 2 as the least. The values of radiated energy per area per time obtained for each region using the two models are not the same, those obtained using model 2 yielded higher values. This is due to the fact that the Gutenberg-Richter constants a and b incorporated into model 2 are approximated values obtained by linear curve fitting which involves extrapolation that is based on the theory that low magnitude events are always under-reported.

In all the regions of study, radiated energy generally increased with time while Gutenberg-Richter constants a and b vary arbitrarily with time and geographical area. This observed increase in radiated energy with time in all the regions studied indicated that there was general increase in seismic activities over the period of time considered. This implies that the lithospheric layer in all the regions of study kept becoming more unstable.

REFERENCES

Abong, A.A., (2007): "Investigation of scale dependence of Gutenberg-Richter's relationship and numerical categorization of seismic activities". M.Sc. thesis submitted to the Department of Physics, University of Ibadan.

Acevedo, A.P.; Bohoroquez, O.P.; Calvache, M.L.; Gil-Cruz,F.; Gomez, D.M.; Londono, J.M.; Ortega, A.; Patino, J. DeJ.; Ponce, A.P.; Rodrigues, S.P.; Sanchez, John J.; Torres, R.A., (2005): "Spatial Mapping of The Galeras Volcano, Colombia, using Earthquakes recorded from 1995 to 2002". Earth Sciences Journal, 06/01/2005.

Adams, R. D. (1976). The Haicheng, China, earthquake of 4 February 1975: the first successfully predicted major earthquake, *Earthquake Eng.Struct. Dynam.* **4,** 423–437.

Agrawal, P.N. (1991). Engineering Seismology New Delhi: Oxford and IBH publishing co pvt Ltd.

Aki, K. (1965): "Maximum likelihood estimate of b in the formular Log N = a - bM and its confidence limits". Bulletin of the Earthquake Research Institute, University of Tokyo, 43, 237 – 239.

Alexander, D. E. (1993): "Natural Disaster" CRC Press (29 July 1993)

Ambraseys, N and Bommer, J. (1990). Uniform magnitude re-evaluation for strong motion database of Europe And Adjacent areas, European Earthquake. Engineering. 2, 3-16.

Amitrano, D. (2003). Brittle-ductile transition and associated seismicity: experimental and numerical studies and relationship with b-value J. Geophis. Res/. 108. ESE 19-1 to 19-15.

Ayele, A. And Kulhanek, O., (1997): "Spatial and temporal variation of seismicity in the horn of Africa from 1960 to 1993. Geophys. J. Int., 130: 805-810

Azeez, O.M and Fasunon, A.O. (1998). Magnitude dependent time series analysis of earthquake flow alonmg the Mid-Atlantic ridge between 10° and 10°S. Contributors in Geophusics. Azeez, O.M.(ed).

Bhatia, S.C., Kumar, M.R., and Gupta, H.K., (2006): "A Probabilistic Seismic Hazard Map of India and Adjoining Regions". Global Seismic Hazard Assessment Program. Retrieved on November 14, 2006.

Blundell, D.J. (1977), Living with Earthquakes, Disasters 1, 41 –6.

Bolt, B.A. (1990). Seismlogy. The encyclopaedia of phusics. New York: Van Nostrand Reinhold. 1089 – 1092.

Dowrick, D.J., (1977): "Earthquake resistant design for Engineers and Architets". 2nd ed. New York; John Wiley and sons.

Drakopoulus, J.C.and Ekonomides, A.C. (1972). Aftershocks of Ferbruary 19, 1968

Earthquake in Northern Aegean Sea and related problems. Pageophy. 95:3

Drakopoulus, J. (1968). Characteristics parameters of Fore- and Aftershocks sequences in the region in Greece. 1- 29 in Drakopoulus, J.C and Ekonomides, A.C.

Eaton, J.P. (1992). Determination of amplitude and Duration magnitudes and site residuals from short period Seismographs in Northern California. Bull. Seismo. Soc. America 82:2.

Encyclopedia Britanica, Ultimate reference suite, (2007): "Earthquakes".

Enescu B, and Ito, K. (2002). Spatial Analysis of the frequency magnitude distribution and decay rate of aftershock activity of the 2000 Western Tottori Earthquake. Earth planets Space, 54, 847-859.

Farell, J., Husen, S., and Smith, R.B., (2008): "b-value mapping of the Yellowstone volcanic and hydrothermal system". Sixty-five Years of b-value Studies I Posters.

Filippo, C. (1897) Cited in (Shearer, 1999). Introduction to seismology. Cambridge: Cambridge University press.

Frohlich, C. And S. Davis (1993): "Teleseismic b-values: Or much ado about 1.0". Journal of Geophysical Research, 98, 631-634.

Geller, R.J. (1976), scaling relations for earthquake source parameters and Magnitudes a Bull. Seismol. Soc. Am. 66, 1501 – 1523.

Gerstenbergeret, M., Wiemer, S. And Gardini, D., (2001). "A systematic test of the hypothesis that the b-value varies with depth in California". Geophys. Res. Let., 28: 57-60.

Gibowicz, S.J. and Lasocki, S., (2001). "Seismicity induced by mining: Ten years later. In: Dmowska, R. and Saltzman, B. (Eds.)", Advances in Geophysics, 44, Academic Press, 39-181.

Gresta, S and Patane, G. (1983). Variation of b values before the Etnean Eruption of March 1981. Pageophy, 121:2. 288 – 295.

Grunthal, G., Hurtig, E. And Ruge, E., (1982). "Time dependence of statistical parameters: the aftershock sequence of the Friuli, Northern Italy, 1976 earthquake and a section of the Montenegro, Yugoslavia, earthquake series 1979". Earthquake Prediction Res., 2: 275-285.

Guidoboni, E. and G. Ferrari (1987): Mallet's macroseismic survey on the Neapolitan Earthquake of 16th December,1857, 4 voll., (Bologna, Italy).

Gutenberg, B. And Richter, C.F., (1942). "Earthquake magnitude, intensity, energy, and acceleration". Bull. Seismol. Am., 32: 163-191.

Gutenberg, B., and C.F. Richter, (1954) Magnitude and energy of earthquakes, Ann. Geof 9, (1), 1-15.

Gutenberg, B. And Richter, C.F., (1954). "In Seismicity of the Earth and associated phenomena". Princeton university Press, Princeton, NJ, USA, 2nd edn.

Gutenberg, B., (1956). "The energy of earthquakes".Quarterly Journal of the Geological Society; 1956; v. 112; issue.1-4; p.1-14; DOI: 0.1144 GSL.JGS.

Gutenberg, B. And Richter, C.F., (1956). "Magnitude and energy of earthquakes". Analli di Geofisica, vol.9, pp.1-15.

Hanks, T.C. and Kanamori, H., (1942). "A moment magnitude scale". Journal of Geophysics Research, 84: 2348-2350.

Hatton, C.G., Main, I.G. and Meredith, P.G., (1993). "A comparison of seismic and structural measurements of scaling exponents during tensile sub-critical crack growth". Journal of structural Geology, 15: 1485-1495.

Hole, K. (1996). Space-time variations of the frequency-energy relation for mining-induced seismicity in the Ostrava-Karvina mining district Pageoph. 146, 265-280.

Holub, K., Šťastná, E. and Trybová, M.: 1994, A revival of seismic activity in broader environs of the town Opava in 1993. Uhlí, rudy a geologický průzkum. Vol. 1, No. 11, 430-435, (in Czech).

Hurtig, E and Stiller, H., (1984): "Erdbeben und Erdbebengerfährdung". Akademiie Verlag Berlin, pp. 328.

Ishimoto, M. and Iida, K. (1939). "Observations of earthquakes registered with the microseismograph constructed recently". Bulletin of the Earthquake Research Institute, University of , Tokyo, 17, 443-478.

Jennings, C.W., (1985). "An explanatory text to accompany the 1:750,000 scale fault and geologic maps of California". California Division of Mines and Geology, Bulletin 201, 197 p.

Jolly, A.D., and McNutt, S.R. (1999): "Seismicity at the volcanoes of Katmai National park, Alaska; July 1995-December 1997". Journal of Vocanology and Geothermal Research, 93, 173-190.

Kagan, Y., (1999): "The universality of the frequency-magnitude relationship". Pure and Applied Geophysics, 155: 537-574.

Kanamori, H., (1977): "The energy released in great earthquakes". Journal of Geophysics Research, 82: 2981-2876.

Karnik, V., Scherkova, Z. , and Schenk, V. (1984). Vulnerability and the MSK Scale, Engineering Geology, 20 161 – 8.

Kitaharak, I. et al. (2003): Documenting Disaster, Natural Disasters in Japanese History, 1703-2003. Nat. Museum of Japanese History, Chiba.

Kulhanek, O., (2005): "Seminar on b-value". Seminar paper, Department of Geophysics, Charles University, Prague.

Lahr, J.C., Chouet, C.D., Stephens, J.A., Power, J.A. and Page, R.A. (1994): "Earthquake classification, location, and error analysis in a volcanic environment environment: implications for the magmatic system of the 1989-1990 eruptions at Redoubt volcano, Alaska". Journal of Volcanology and Geothermal Research, 62: 1-4, 137-151.

Lay, T., H. Kanamori, C. J. (2005): "The Great Sumatra-Andaman Earthquake of 26 December 2004". Science, 20 May, 1127–1133, 2005.

Linzer, L.M., (2006): A summary of recent research in seismology in South Africa.

Lockner, D.(1996): "Brittle fracture as an analog to earthquakes: Can acoustic emission be used to develop a viable prediction strategy". Journal of acoustic Emission, 14: S88-S101.

Lowrie, W. (1997). Fundamentals of Geophysics. Cambridge: Cambridge University Press.

Main I.G., Peacock S. and Meredith P.G. (1990): "Scattering attenuation and the fractal geometry of fracture systems". Birkäuser Basel, vol.2, number 2.

Main, I.G., Colombo, I.G. and Ford, M.C., (2003): "Assessing damage of reinforced concrete beam using b-value analysis of acoustis emission signal". Journal of Material and Civil Engineering, 15: 280-286.

McGarr, A., (1984): "Some application of seismic source mechanism studies to assess underground hazard. In: N.C. Gay and E.H. Wainwright(Eds.)". Proc. 1st Inter. Congress on Rockbursts and Seismicity in Mines. SAIM Johennesburg, pp. 199-208.

McNally, K.C., (1989): Earthquakes and siesmicity. In: D.E. James(Ed.): "The Encyclopedia of Solid Earth Geophysics, pp. 308-315.

Minakami. T. (1974). Seismology of Volcanoes in Japan. Civetta, L, gasparini, P, Lunong, G and Rapolla, A. Eds. Physical volcanology. Amsterdam: Elsevier, 1-27.

Mogi, K., (1962): “Magnitude-frequency relationship for elastic shocks accompanying fractures of various materials and some related problems in earthquakes”. Bulletin of Earthquake Research Institute, University of Tokyo, 40: 831-883.

Molchan, G.M and Dmitrieve. (1990). Dynamics of magnitude frequency relation of aftershocks. Phys. Earth Planet. Inter., 61, 99-112.

Molchan, G.M, T, L. Kronrod, and A.K Nekrasova. (1999). Immediate foreshocks: Time Variation of the b-value. Phys. Inter.111, 229-240.

Monterroso, D. And Kulhanek, O., (2003): “Spatial variations of b-values in the subduction zone of central America”. Geofisica Inter. 42: 1-13.

Monterroso, D., (2003): “Seismic precursory potential of temporal variation of b-value: five case studies in Central America”. Comprehensive Summaries of Uppsala Disertations from the Faculty of Science and Technology, 897, pp.17.

Mori, J and Abercrombie, R.E. (1997). Depth dependence of Earthquakes frequency-magnitude distribution in California: Implications for future Initiation. Geophysical Research Journal. 102, 15, 081-15, 090.

Murru, M. and Lisi, A., (2008): “Mapping of anomalies in tectonic zone (central Italy) and beneath Mt. Etna volcano (Sicily, Italy)”. Sixty-five Years of b-value Studies I Posters.

Nakaya, S. (2004). A zone of anomalously low b-value within the subduction slab prior to the September 26, 2003. Tokachi-Oki, Japan, earthquake (M=8.0), EOS Trans. AGU, 85:47, Fall meeting suppl Abstract S13Am 1028.

Nuannin, P., Kulhanek, O., Persson, L. And Tillman, K., (2002): “Forecasting of increasing induced seismicity in the Zinkgruvan mine, Sweden, by temporal variations of b-values”. Acta Montana, Series A, 21: 13-25.

Nuannin, P., Kulhanek, O., Persson, L. (2005): “Spatial and temporal b-value anomalies preceding the devastating off coast of NW Sumatra earthquake of December 26, 2004”. Geophysics research Lecture, 32, L11307.

Ogata, Y., M. Imoto, and K. Katsura, (1991). 3-D spatial variation of b-values of magnitude frequency distribution beneath the Kanto district, Japan, J Geophys. Int., 104, 135-146.

Onuoha, M. K. (2001). Foundation postgraduate course in Theoretical Geophysics. National Mathematical Centre, Abuja.

Pacheco, J.F., Scholz, C.H. and Skyes, L.R., (1992): “Changes in frequency-size relationship from small to large earthquakes. Nature, 335: 71-73.

Paiboon, N. (2006). The potential of b-value variations as earthquake precursors for small and large events. Digital comprehensive summaries of Uppsala dissertations from the faculty of science an technology. 183.

Papazachos, C., (1999): “An alternative method for a reliable estimation of seismicity with an application in Greece and the surrounding area”. Bulletin of the seismological society of America. February 1999, v.89; no. 1, pp. 111-119.

Popoola, I.O., (2008) : “Introduction to seismology (Phy 713)”. Lecture notes, Department of Physics, University of Ibadan.

Rao, M.V.M.S., Murphy, D.N.S., Nagaraja Rao, G.M., Mohananty, S.K. and Udaya Kumar, S. (2004) : “Stress-induced micro-cracking and brittle failure of Godhra granite”. Journal of geological Society of India, 64, 775-783.

Rao, M.V.M.S., and Prasanna Lashimi, K.J., (2005): “Analysis of b-value and improved b-value of acoustic emissions accompanying rock fracture”. Current science, vol.89, no. 9.

Richter, C.F. (1935). An instrumental earthquake magnitude scale. Bull. Seismol Soc. Am., 25, 1-32.

Sammonds, P.R., Meredith, P.G., and Main, I.G. (1999): “Role of pore-fluids in the generation of seismic precursors to shear fracture”. Nature, 359 : 228-230.

Scholz, C.H., (1968): “The frequency-magnitude relation of microfracturing in rocks and its relation to earthquakes”. American Seismological Society Bulletin 58: 399-415.

Schorlemmer, D., S. Wiemer, M. Wyss, and D. D. Jackson (2004), Earthquake statistics at Parkfield: 2. Probabilistic forecasting and testing, *J. Geophys. Res.*, 109, B12308, doi:10.1029/2004JB003235.

Schwartz, D.P., (1988): “Geology and seismic hazards : Moving into the 1990’s”. Pro. ASCE conf. “Earthquake Engineering and Soil Dynamics II”, 1-42.

Shearer, Peter M., (1999): “Introduction to seismology”. Cambridge University Press, UK. ISBN 0 521 66023 8.

Steacy, S.J., J. McCloskey, C.J. Bean and J. Ren (1996), Heterogeneity in a self-organized critical earthquake model, Geophysical Research Letters, *23, 383-386.*

Stein, S., Wysession, M., (2003): An introduction to seismology, earthquakes, and earth structure. Wiley-Blackwell. ISBN 0-86542-078-5.

Suyehiro, S., Asada, T. And Ohtake, M., (1964): “Foreshocks and aftershocks accompanying a perceptible earthquake in central Japan: On the peculiar nature of foreshocks”. Pap. Metrol. Geophys., 19: 427-435.

Udias, A. and Mezcua, J., (1997): "Fundamentos de Geofisca. Alianza Universidad Textos, pp. 476.

Urbancic, T. I., C. I. Trifu, J. M. Long, and R. P. Young (1992), Space-time correlations of b-values with stress release, Pure Appl. Geophys., 139, 449– 462.

Utsu, T., (1965): "A method for determining the value of b in the formular logN=a-bM showing the manitude frequency relation for earthquakes". Geophys. Bull. Hokkaido Univ., 13: 99-103.

Wadati, K., (1931) Shallow and Deep Earthquakes (3rd paper), Geophysical Mag., Vol. 4, pp. 231 – 283, Tokyo.

Warren, N.W. and Latham, G.V., (1970): "An experimental study of thermal induced microfracturing and its relation to volcanic seismicity". Journal of geophysics research, 75: 4455-4464.

Wiemer, S. And Benoit, J., (1996): "Mapping the b-value anomaly at 100km depth in the Alaska and New Zealand subduction zones". Geophys. Res. Let., 23: 1557-1560.

Wiemer, S., McNutt, S.R. and Wyss, M., (1998): "Temporal and three-dimensional spatial analyses of the frequency-magnitude distribution near Long Valley Caldera, California". Geophysics journal international, 134: 409-421.

William, S., Sipkin, S. A., Choy, G. L., (1989): "Measuring the Size of an Earthquake". United States Geological Survey.

Wood, H.O. & Neumann, F (1931). Modified Mercalli Intensity scale of 1931. Bulletin of the Seismological Society of America, 21: 277 – 283

www.ncedc.org/anss/catalog-search.html

Wyss, M., (1973): "Towards a physical understanding of the earthquake frequency distribution". Geophys. J.R. astr. Soc., 31: 341-359.

United State Geological Survey, Magnitude.http://www.usgs.gov/earthquakes

APPENDIX